

*ARMY RESEARCH LABORATORY*



## **FPI and MPI of Cracks Under Coatings**

**by Scott Grendahl and Benjamin Hardisky**

**ARL-TR-4033**

**January 2007**

## **NOTICES**

### **Disclaimers**

The findings in this report are not to be construed as an official Department of the Army position unless so designated by other authorized documents.

Citation of manufacturer's or trade names does not constitute an official endorsement or approval of the use thereof.

Destroy this report when it is no longer needed. Do not return it to the originator.

# **Army Research Laboratory**

Aberdeen Proving Ground, MD 21005-5069

---

---

**ARL-TR-4033**

**January 2007**

---

---

## **FPI and MPI of Cracks Under Coatings**

**Scott Grendahl and Benjamin Hardisky**  
**Weapons and Materials Research Directorate, ARL**

<b>REPORT DOCUMENTATION PAGE</b>			<i>Form Approved</i> OMB No. 0704-0188		
Public reporting burden for this collection of information is estimated to average 1 hour per response, including the time for reviewing instructions, searching existing data sources, gathering and maintaining the data needed, and completing and reviewing the collection information. Send comments regarding this burden estimate or any other aspect of this collection of information, including suggestions for reducing the burden, to Department of Defense, Washington Headquarters Services, Directorate for Information Operations and Reports (0704-0188), 1215 Jefferson Davis Highway, Suite 1204, Arlington, VA 22202-4302. Respondents should be aware that notwithstanding any other provision of law, no person shall be subject to any penalty for failing to comply with a collection of information if it does not display a currently valid OMB control number. <b>PLEASE DO NOT RETURN YOUR FORM TO THE ABOVE ADDRESS.</b>					
<b>1. REPORT DATE (DD-MM-YYYY)</b> January 2007		<b>2. REPORT TYPE</b> Final		<b>3. DATES COVERED (From - To)</b> 1 June 2005–12 July 2006	
<b>4. TITLE AND SUBTITLE</b> FPI and MPI of Cracks Under Coatings			<b>5a. CONTRACT NUMBER</b>		
			<b>5b. GRANT NUMBER</b>		
			<b>5c. PROGRAM ELEMENT NUMBER</b>		
<b>6. AUTHOR(S)</b> Scott Grendahl and Benjamin Hardisky			<b>5d. PROJECT NUMBER</b> 581P31		
			<b>5e. TASK NUMBER</b>		
			<b>5f. WORK UNIT NUMBER</b>		
<b>7. PERFORMING ORGANIZATION NAME(S) AND ADDRESS(ES)</b> U.S. Army Research Laboratory ATTN: AMSRD-ARL-WM-MC Aberdeen Proving Ground, MD 21005-5069			<b>8. PERFORMING ORGANIZATION REPORT NUMBER</b> ARL-TR-4033		
<b>9. SPONSORING/MONITORING AGENCY NAME(S) AND ADDRESS(ES)</b> U.S. Army Aviation and Missile Command Redstone Arsenal, AL 35898			<b>10. SPONSOR/MONITOR'S ACRONYM(S)</b> AMCOM		
			<b>11. SPONSOR/MONITOR'S REPORT NUMBER(S)</b>		
<b>12. DISTRIBUTION/AVAILABILITY STATEMENT</b> Approved for public release; distribution is unlimited.					
<b>13. SUPPLEMENTARY NOTES</b>					
<b>14. ABSTRACT</b> The U.S. Army Aviation and Missile Research Development and Engineering Center requested that the U.S. Army Research Laboratory develop and execute a program designed to evaluate the performance of nondestructive inspection (NDI) techniques over typical army aviation paint systems. Corpus Christi Army Depot performs the majority of the current maintenance and overhaul operations on army aviation systems. This facility would greatly benefit in throughput and in reduction of hazardous waste generated if the removal of the applied coating systems could be avoided. The objective of this work was to evaluate the effect of not removing the most common currently approved aviation coating system on the NDI cycles. The test plan and methodology was created in conjunction with and approved through AMSRD-AMR-AE-F-M.					
<b>15. SUBJECT TERMS</b> flashjet, rotor-blade composite, mechanical properties					
<b>16. SECURITY CLASSIFICATION OF:</b>			<b>17. LIMITATION OF ABSTRACT</b>  UL	<b>18. NUMBER OF PAGES</b>  72	<b>19a. NAME OF RESPONSIBLE PERSON</b> Scott Grendahl
<b>a. REPORT</b> UNCLASSIFIED	<b>b. ABSTRACT</b> UNCLASSIFIED	<b>c. THIS PAGE</b> UNCLASSIFIED			<b>19b. TELEPHONE NUMBER (Include area code)</b> 410-306-0819

---

## Contents

---

<b>List of Figures</b>	<b>v</b>
<b>List of Tables</b>	<b>vii</b>
<b>1. Background</b>	<b>1</b>
<b>2. Development of the Test Plan</b>	<b>1</b>
<b>3. Materials Selection and Procurement</b>	<b>3</b>
<b>4. Background of Fatigue-Generated Cracks</b>	<b>3</b>
4.1 Bar Preparation.....	4
4.2 Crack Initiation and Extension.....	4
4.3 Creation of Fatigue Cracks.....	5
4.4 Light Optical Photometer.....	12
<b>5. Materials Pretreatment</b>	<b>12</b>
<b>6. FPI/MPI and Light Measurements</b>	<b>12</b>
<b>7. Painting</b>	<b>13</b>
<b>8. Crack Extension After Painting</b>	<b>13</b>
<b>9. Plastic Media Blasting</b>	<b>14</b>
<b>10. Chemical Removal of Paint</b>	<b>16</b>
<b>11. Results</b>	<b>16</b>
11.1 Aluminum.....	16
11.2 Titanium.....	20
11.3 Magnesium.....	25
11.4 Steel.....	33

<b>12. Discussion</b>	<b>38</b>
12.1 Scope .....	38
12.2 Effect of Performing FPI Over Paint.....	38
12.3 PMB.....	39
12.4 Chemical Removal .....	39
<b>13. Conclusions</b>	<b>39</b>
13.1 FPI .....	39
13.2 MPI.....	39
<b>14. References</b>	<b>40</b>
<b>Appendix. Schematics of the Incremental Formation of the Specimens</b>	<b>41</b>
<b>Distribution List</b>	<b>60</b>

---

## List of Figures

---

Figure 1. Flow diagram for evaluating FPI and MPI of cracks under coatings.....	2
Figure 2. Schematic of the cross section of a typical fatigue-cracked test specimen depicting the incremental removal of material from the top surface and its corresponding effect on crack-length reduction. ....	11
Figure 3. Al bar no. 7 after initiation and extension (shows crack at its final length.).....	18
Figure 4. FPI of Al bar no. 7 after initiation and extension. ....	18
Figure 5. Al bar no. 7 illustrating the manner in which the brightness measurements were acquired. The top dot represents the area the spotmeter was focused for the background measurement, and the bottom dot represents the area from which the crack measurement was acquired.....	19
Figure 6. FPI of Al bar no. 7 crack after anodizing. ....	19
Figure 7. FPI of Al bar no. 7 crack after painting.....	20
Figure 8. FPI of Al bar no. 7 after PMB. The crack can be observed visually, but no indication can be observed.....	21
Figure 9. FPI of Al bar no. 7 performed after the bar had been processed in paint stripper and after the bar had been mechanically flexed.....	21
Figure 10. FPI of Al bar nos. 8, 9, and 10—the bars with cracks extended ~0.050 in after painting—performed after the bars had been painted and the cracks mechanically flexed.....	22
Figure 11. Titanium bar no. 6—0.1-in crack after initial crack extension.....	22
Figure 12. FPI of titanium bar no. 6—0.1-in crack after initial crack extension.....	24
Figure 13. FPI of titanium bar no. 6 showing areas where brightness measurements were taken. The top spot is the brightness of the crack, and the bottom spot (below the crack) is where the background reading was taken. ....	24
Figure 14. FPI of titanium bar no. 6 after painting. ....	25
Figure 15. FPI of titanium bar no. 6 after the painted bar had been extended by 0.5 in.....	26
Figure 16. Optical micrograph of titanium bar no. 6 showing the extended crack after PMB.....	26
Figure 17. FPI micrograph of titanium bar no. 6 after PMB and mechanical flexing. Initial FPI produced no visible indication after PMB. ....	27
Figure 18. FPI micrograph of titanium bar no. 6 after PMB and chemical-stripper processing. The results are similar to those after painting and crack extension. ....	27
Figure 19. Magnesium bar no. 2 with a 0.2-in crack length. ....	29
Figure 20. FPI micrograph of cracked Mg bar no. 2 after the crack was initiated and extended to the desired length.....	29

Figure 21. FPI micrograph of cracked Mg bar no. 2 depicting the typical locations of the light measurements. The top spot is the brightness of the crack, and the bottom spot (below the crack) is where the background reading was taken. ....	30
Figure 22. FPI micrograph of cracked Mg bar no. 2 after the Tagnite coating. ....	30
Figure 23. FPI micrograph of cracked Mg bar no. 2 after the application of the coating system. No crack can be observed, and the absorption of the penetrant by the coating is evident. ....	31
Figure 24. FPI micrograph of cracked Mg bar nos. 3, 6, and 7 after crack extension under the coating system. Cracks can be observed; however, the absorption of the penetrant by the coating is still evident. ....	32
Figure 25. Typical FPI results after PMB, chemical processing, and mechanical flexing to remove the plastic media from within the cracks. Results shown for Mg bar no. 2 after soaking in paint stripper ~24 hr. ....	32
Figure 26. Typical FPI results after crack extension under the coating, PMB, mechanical flexing, and chemical-stripper processing. Results shown for Mg bar nos. 3, 6, and 7 after soaking in paint stripper ~24 hr. ....	33
Figure 27. Bar no. 3 after initiation and crack extension—typical fatigue crack generated in steel. ....	35
Figure 28. Steel bar no. 6 after initial crack extension—0.2 in crack. Typical FPI visual results on steel fatigue cracks. ....	35
Figure 29. Typical FPI micrograph of steel showing the areas where brightness measurements were taken on this bar. The top dot (on the crack) is the crack brightness measurement location. The bottom dot (below the crack) is the background measurement location. ....	36
Figure 30. Bar no. 6 after the initiation and crack extension. Typical baseline visual MPI micrograph on steel. ....	36
Figure 31. Bar no. 6 after the 0.050-in crack extension. Typical visual MPI micrograph after crack extension. ....	37
Figure 32. Typical visual MPI micrograph after the application of the second layer of paint. All traces of the crack indication are gone. ....	37

---

## List of Tables

---

Table 1. Polishing, crack initiation, and crack extension data for aluminum bars. ....	6
Table 2. Polishing, crack initiation, and crack extension data for magnesium bars. ....	7
Table 3. Polishing, crack initiation, and crack extension data for titanium bars. ....	7
Table 4. Polishing, crack initiation, and crack extension data for steel bars. ....	8
Table 5. Aluminum grinding data. ....	9
Table 6. Magnesium grinding data. ....	9
Table 7. Titanium grinding data. ....	10
Table 8. Steel grinding data. ....	11
Table 9. Data after paint crack extension. ....	15
Table 10. Aluminum spotmeter readings. ....	17
Table 11. Titanium spotmeter readings. ....	23
Table 12. Magnesium spotmeter measurement. ....	28
Table 13. Steel spotmeter measurements. ....	34

INTENTIONALLY LEFT BLANK.

---

## 1. Background

---

The U.S. Army Aviation and Missile Research Development and Engineering Center (AMRDEC) requested that the U.S. Army Research Laboratory (ARL) develop and execute a program designed to evaluate the performance of nondestructive inspection (NDI) techniques over typical army aviation paint systems. Corpus Christi Army Depot performs the majority of the current maintenance and overhaul operations on army aviation systems. This facility would greatly benefit in throughput and in reduction of hazardous waste generated if the removal of the applied coating systems could be avoided. The objective of this work was to evaluate the effect of not removing the most common currently approved aviation coating system on the NDI cycles. The test plan and methodology was created in conjunction with and approved through AMSRD-AMR-AE-F-M.

---

## 2. Development of the Test Plan

---

The test plan was developed by utilizing the prior research and development of Aeronautical Design Standard 61, ADS-61-PRF (1), specifically those sections dealing with fluorescent penetrant inspection (FPI) method, the creation of standardized cracks in specific sizes, and nonbiased, quantitative, light photometer measurement. A flow chart is provided for reference purposes (figure 1) and the test matrix is summarized as follows:

- Objective: Evaluate the effect of surface paint systems on FPI and magnetic particle inspection (MPI) performance in aviation maintenance and overhaul operations.
- Materials/Condition: 2024-T3 Al anodized in accordance with (IAW) MIL-A-8625 (2) prior to painting, bare Ti-6-4, AZ31B Mg Tagnite\* -coated prior to painting, and cadmium-plated 4340 steel IAW SAE-AMS-QQ-P-416 (3) at a 40–50 Rockwell hardness (HRC) level.
- Test Specimens: The specimens were utilized to generate fatigue cracks of a known size. Three sizes for each material were used: 0.025, 0.1, and 0.2 inches in length. Two samples at each length for each material were used. Specimens have typical machined surface finishes.
- Geometry: 1- × 6- × 0.4-in flat specimens. There is no reason to believe a flat surface isn't the worst case for crack detection.

---

\*Tagnite is a registered trademark of Technology Applications Group.

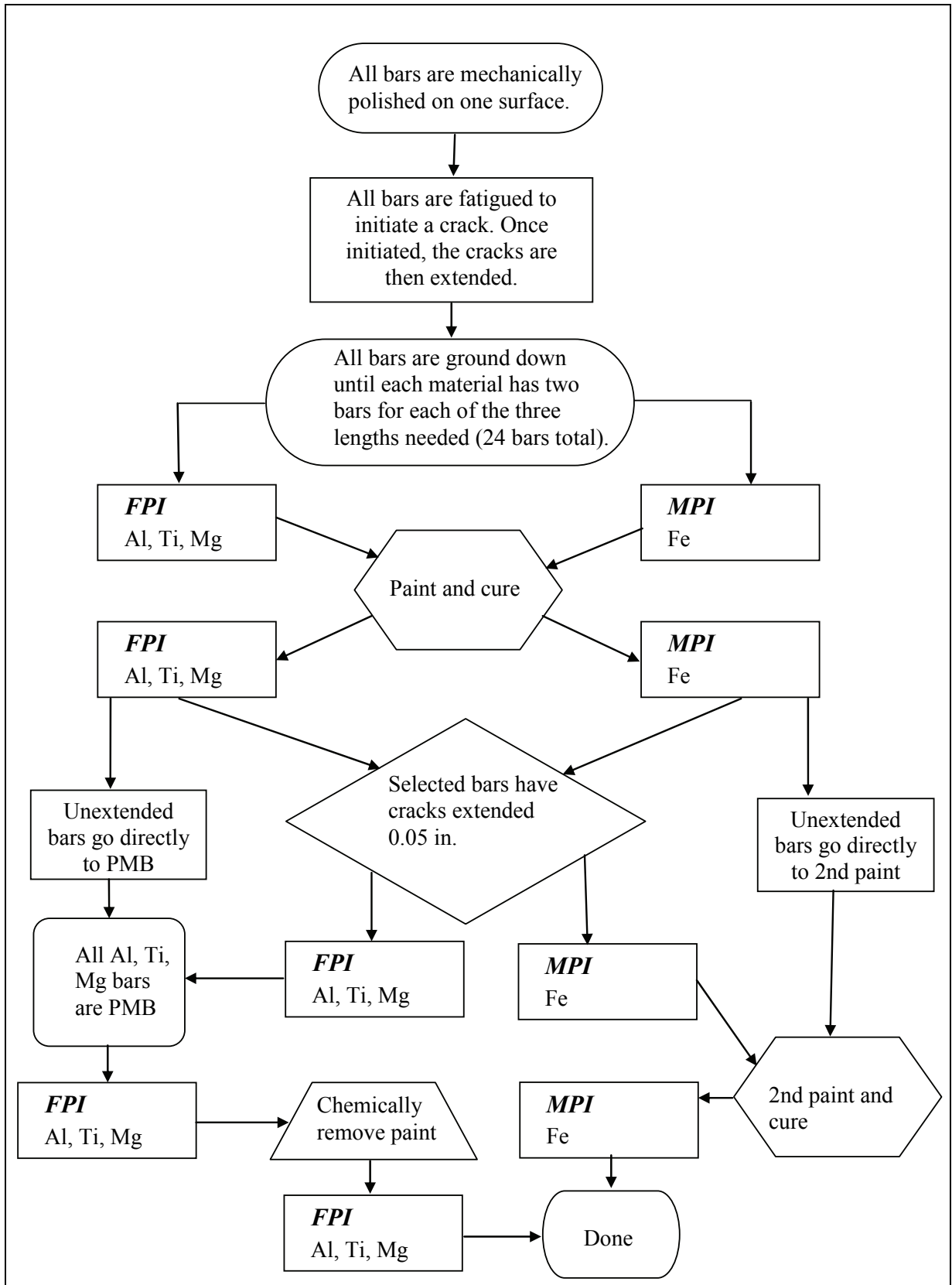


Figure 1. Flow diagram for evaluating FPI and MPI of cracks under coatings.

- Primer: Epoxy primer (MIL-P-23377 [4], Type II, Class C) to dry film thickness of 1–1.5 mil.
  - Topcoat: New chemical agent resistant coating (CARC), MIL-C-64159 (5), to a dry film thickness of 2–2.5 mil. Apply MPI coating in layers to evaluate the results incrementally.
  - Drying Conditions: Air-dry the primed and painted specimens for 1 week, and then bake the specimens at 150 °F for 1 week.
  - Cleaning: Simulate conventional maintenance cleaning cycles prior to FPI inspection.
  - FPI: IAW the standard method of ADS-61-PRF.
  - MPI: IAW ASTM-E-1444 (6). After performing baseline MPI, paint and cure the three cracked test specimens with conventional operations. Perform MPI again after the paint and cure cycle. Add additional paint thickness and cure cycles while performing MPI in between stages. Record coating thickness and record observations with text and photographs. Determine the thickness at which MPI becomes detrimentally affected. Cycle cracks to extend ~0.050 in. Repeat MPI cycle to determine the thickness at which MPI becomes detrimentally affected.
- 

### **3. Materials Selection and Procurement**

---

Four U.S. Army aviation relevant materials were selected to be incorporated into the test protocol. These materials were 2024-T3 Al anodized IAW MIL-A-8625 prior to painting, bare Ti-6-4, AZ-31B Mg Tagnite-coated prior to painting, and cadmium-plated 4340 steel IAW SAE-AMC-QQ-P-416 at 40–50 HRC. Twenty samples of each material were procured. The specimen size was 1 × 0.4 × 6 in. These specimens were utilized to generate fatigue cracks.

---

### **4. Background of Fatigue-Generated Cracks**

---

These precracked test bars are not off-the-shelf items. Typical nondestructive testing (NDT) standards incorporate thin aluminum or chrome-plated substrates pressure-dimpled from the back side or electrically discharged (sparked) to generate cracks on the front side of the plates. Various crack sizes can be generated from these methods, but they are not “tight” because of their inherent material properties (low modulus of elasticity) and the fact that they are not generated from metal fatigue cycling. There are also NDT test specimens that contain electro-discharge machining slots that also do not have the same tight geometry as fatigue cracks and are limited in their usefulness. When performing FPI on aircraft components, and especially when

inspecting helicopters, fatigue cracks are the main concern. The sizes of the cracks were predetermined by AMRDEC and based upon previous research and risk concerns. The concept behind the original crack-size determination is that the smallest crack size reliably observable by the utilized technique must be determined (in this case by FPI and MPI), and then that crack size is used to verify that any process modification (such as the process being performed over paint) does not detrimentally effect the observation of an indication. In this case, an  $\sim 0.025$ -in crack is the smallest detectable (at a 95% probability of detection [POD] level), and cracks of  $\sim 0.05$  in should be readily observable and distinct at the 100% POD level. Cracks of 0.1 in and 0.2 in are considered large for these techniques and also should not be overlooked. They were included to provide a measure of any detrimental effect.

#### **4.1 Bar Preparation**

For several reasons, the bars needed to be mechanically finished prior to exposure to cyclic fatigue. During the extension process, the crack had to be observable in order to approximate its length and in order to prevent the crack from reaching a critical length and undergoing catastrophic failure. This required a surface finish smoother and more polished than a normal rolled plate finish. One of the  $6 \times 1$ -in surfaces and the two adjacent side surfaces of each bar were ground, in most cases with 4000-grit silicon carbide paper. The grinding was done on a Buehler Ecomet 4 variable speed grinder/polisher. To prevent edge cracks from forming, the edges required an  $\sim 0.1$ -in edge break from 4000-grit silicon carbide paper to reduce the stress concentration effects of the sharp edge. Manually polishing an item the size of these bars is no small matter. A refined technique was needed to keep the bars flat and parallel while providing the surface finish required over the large area. Even with this surface finish, several bars initiated cracks at an edge before generation occurred at an induced flaw in the center of the  $6 \times 1$ -in surface.

#### **4.2 Crack Initiation and Extension**

All fatigue testing was done on an Instron 1332 servo hydraulic testing machine with an 8500 plus controller. An MTS three-point and four-point bend fixture, in combination with rollers sized in accordance with the loading required, was used for all cyclic fatigue. The four-point bend fixture was used for all crack initiation and extension. The three-point bending fixture was used during the extension of the cracks after the bars were painted. A small scratch from a razor blade was placed in the center of each bar prior to cyclic fatigue (because of the hardness of steel and titanium, a diamond-tipped indenter was required for those specimens). This scratch created a local defect which acted as a stress concentration site, increasing the likelihood that initiation would take place in the center of the bar. The loop-shaping parameters for the closed-loop servohydraulic monitoring were adjusted to provide optimum cycling conditions. Using the four-point bending calculation equation and the four-point critical stress intensity equation, the loads required to initiate and extend a crack were calculated for each of the test materials.

Four-Point Bending Calculation:

$$\sigma = \frac{(3PL)}{(4bd^2)}, \quad (1)$$

where

$P$  = load,  
 $L$  = outer span,  
 $b$  = width,  
 $p$  = thickness, and  
 $\sigma$  = stress.

Four-Point Critical Stress Intensity Equation:

$$\frac{3}{2} \frac{P(S_1 - S_2)}{BW^{3/2}} x \left( \frac{ax\pi}{W} \right)^{1/2} xf(a/W), \quad (2)$$

where

$S$  = span,  
 $a$  = crack length,  
 $W$  = specimen thickness, and

$$f(a/W) = \frac{3(a/W)^{1/2} [1.99 - (a/W)(1 - a/W)x(2.15 - 3.93a/W + 2.7a^2/W^2)]}{2(1 + 2a/W)(1 - a/W)^{3/2}}. \quad (3)$$

Tables 1–4 present the polishing, crack initiation, and crack extension data for the four materials. During crack initiation, the scratch was observed with a flashlight until a visible crack was evident. Visible dye penetrant was utilized on the scratches of some specimens to assist in the detection of crack initiation and progression. The specimen was then removed from the machine, and the crack was measured via optical microscopy. Once the crack length was determined, it was further cyclically loaded with adjusted loading parameters that favored high cycle fatigue. The crack was once again observed with a flashlight until it had extended to a length of ~0.25 in. At this point, the crack was considered acceptable for preparation of its final length.

The crack depths were then estimated using an eddy current crack detection unit. By using the crack depth and length, accurate “thumbnail” models of the crack cross sections could be drawn. This helped estimate how much material to remove during the next step in order to reduce the length of the cracks to the desired amount.

### 4.3 Creation of Fatigue Cracks

Although the test matrix calls for only six fatigue-cracked specimens of each material, generating cracks of a known size on the open face plane (not an edge or a corner) of a material is considerably tedious and involves a multitude of specimens for destructive evaluation. Some

Table 1. Polishing, crack initiation, and crack extension data for aluminum bars.

Bar No.	Polish Before Cycling (SiC grit)	R Value	Cycling Load (lb)	(±) (lb)	Cycles	Result
1	1000	0.28	3575	2000	2000	No crack
		0.28	3575	2000	000	No crack
		0.28	3575	2000	10,000	Cracked, but also has edge crack
2	1000	0.28	3575	2000	10,000	No crack
		0.28	3575	2000	10,000	Cracked, but also has edge crack
		0.33	2000	1000	10,000	Extended to ~0.34 in
3	1000	0.28	3575	2000	14,000	Catastrophic fracture
4	1000	0.28	3575	2000	13,000	Catastrophic fracture
5	4000	0.41	3575	1500	13,000	Cracked ~0.2 in
		0.25	1000	600	50,000	Extended to ~0.26 in
6	4000	0.41	3575	1500	13,000	Cracked ~0.25 in
		0.25	1000	600	32,000	Extended to ~0.275 in
7	4000	0.41	3575	1500	5000	No crack
		0.41	3575	1500	6400	Cracked ~0.3 in
		0.2	1500	1000	7000	Extended to ~0.4 in
8	4000	0.41	3575	1500	16,500	Cracked ~0.21 in
		0.25	1250	750	10,000	Extended to ~0.275 in (curved)
9	4000	0.48	3575	1250	10,000	No crack
		0.41	3575	1500	10,000	No crack
		0.28	3575	2000	5000	Cracked ~0.25 in
		0.25	1000	600	40,000	Extended to ~0.325 in
10	4000	0.41	3575	1500	10,000	No crack
		0.41	3575	1500	5000	Cracked ~0.2 in
		0.25	1000	600	40,000	Extended to ~0.275 in

Note:      Indicates that the bar was later used for FPI measurements.

cracks must be opened destructively to insure that the cyclic loading utilized is generating a uniform, semicircular, thumbnail surface crack. All the materials were bare during crack initiation and extension and pretreated before painting. The generation of the cracks involves many steps: initiating a precrack in the correct location, growing that precrack to a size larger than that which is desired, and grinding and polishing the specimen faces until the cracks are the correct sizes. Issues arise when attempting to achieve a specific crack length. In the case of this test matrix, three sizes were selected: 0.2, 0.1, and 0.025 in. In each case, a specific step-by-step procedure was followed. Grinding removed material from the cracked surface of the test specimens. All of the grinding was performed on a Mark surface grinder. The grinding data is presented in tables 5–8. The specimens were then hand-polished to remove the smeared material from the grinding step (the removal is never uniform; it is a function of grinding parameters and the number of specimens being ground). The polishing was performed on a Buehler Ecomet 4

Table 2. Polishing, crack initiation, and crack extension data for magnesium bars.

Bar No.	Polish Before Cycling (grit)	R Value	Cycling Load (lb)	(±) (lb)	Cycles	Result
1	4000	0.1	687.5	562.5	20,000	No crack
		0.1	750	625	10,000	No crack
		0.11	875	700	7500	Cracked 0.225 in
		0.14	400	300	20,000	Extended to 0.25 in
2	4000	0.11	875	700	10,000	Cracked 0.14 in
		0.14	400	300	150,000	Extended to 0.275 in
3	4000	0.11	875	700	10,000	Cracked 0.12 in
		0.14	400	300	90,000	Extended to 0.25 in
			550	450	15,000	
4	4000	0.11	875	700	10,000	Cracked 0.18 in
		0.14	400	300	70,000	Extended to 0.22 in
5	4000	0.11	875	700	10,000	Cracked 0.185 in
		0.14	400	300	80,000	Extended to 0.255 in
6	4000	0.11	875	700	10,000	Cracked 0.15 in
		0.14	400	300	75,000	Extended to 0.26 in
		0.1	550	450	10,000	
7	4000	0.1	825	675	20,000	Cracked 0.09 in
8	4000	0.1	825	675	33,000	Cracked 0.09 in

Note:      Indicates that the bar was later used for FPI measurements.

Table 3. Polishing, crack initiation, and crack extension data for titanium bars.

Bar No.	Polish Before Cycling (grit)	R Value	Cycling Load (lb)	(±) (lb)	Cycles	Result
1	1200	0.1	6600	5400	4000	Broke at 4000
2	1200	0.1	5500	4500	10,000	No crack
		0.1	5500	4500	4000	No crack
		0.1	5500	4500	5000	Broke at edge crack
3	1200	0.1	5500	4500	7500	Cracked 0.23 in
4	1200	0.1	5500	4500	10,000	No crack
		0.1	5500	4500	6700	Cracked 0.17 in
		0.1	3000	2500	20,000	No extension
		0.1	4000	3250	2500	Cracked 0.28 in
5	1200	0.1	5500	4500	10,000	No crack
		0.1	5500	4500	4872	Three edge cracks observed, small crack in the groove
6	1200	0.1	5500	4500	10,000	No crack
		0.1	5500	4500	1200	Cracked 0.295 in
7	1200	0.1	5500	4500	8300	Cracked 0.25 in
8	1200	0.1	5500	4500	13,500	Cracked 0.28 in
9	1200	0.1	5500	4500	10,000	Cracked 0.28 in

Note:      Indicates that the bar was later used for FPI measurements.

Table 4. Polishing, crack initiation, and crack extension data for steel bars.

Bar No.	Polish Before Cycling (grit)	R Value	Cycling Load (lb)	(±) (lb)	Cycles	Result
1	4000	0.1	6600	5400	7000	Short crack ~0.11 in
		0.45	6600	2500	8000	Extended to 0.25 in
2	4000	0.1	6600	5400	11,000	Cracked 0.18 in
		0.45	6600	2500	5500	Extended to 0.275 in
3	4000	0.1	6600	5400	7500	Short crack
		0.45	6600	2500	7000	Extended to 0.25 in
4	4000	0.1	6600	5400	10,000	Short crack
		0.32	6600	3400	3600	Extended to 0.225 in
5	4000	0.1	6600	5400	8000	Cracked 0.18 in
		0.45	6600	2500	5500	Extended to 0.25 in
6	4000	0.1	6600	5400	5600	Short crack, barely noticeable
		0.45	6600	2500	12,000	Extended to 0.225 in

Note:  Indicates that the bar was later used for MPI measurements.

with silicon carbide paper. Then, the specimens were examined with optical microscopy and scanning electron microscopy in conjunction with FPI to determine the actual crack length. This procedure was repeated incrementally until all the specimens had the correct crack lengths. In all, six specimens of each material were precracked, with two specimens for each crack length. Testing the lower limit of detectability of FPI and MPI (0.025 in) proved extremely difficult. Quite often, the 0.025-in cracks were polished away in an attempt to reduce the size of a longer crack. The removal of even minute amounts of material at the crack front of a thumbnail crack has a considerable impact on crack length. The final stage in specimen fabrication proved to be even more disconcerting. It is important that the specimens do not have a polished smooth surface. Instead, they should have a surface consistent with the components they represent, i.e., typical aviation parts. Therefore, the final step was to provide the specimens with a typical 125 root-mean-square surface finish. This surface finish was applied with a Buehler belt grinder with 225-grit paper. The application of this surface finish removes a great deal of material and must be accounted for before finalizing the crack size. If it isn't, the smallest cracks are completely removed during this process. Once the cracks had the correct lengths, nondestructive inspection (NDI) was performed on the bars, and fluorescent light measurements were taken to get baseline values. FPI was performed on the aluminum, magnesium, and titanium, and MPI was performed on the steel. Subsequent to the baseline measurement, all bars except the titanium were pretreated with their respective coatings. Schematics of the incremental grinding and polishing for each of the specimens can be found in the appendix. The schematics in the appendix represent only the crack plane and are an enlargement of the cross section of the component (figure 2).

Table 5. Aluminum grinding data.

Bar No.	Machine Removed	0.01	0.05	0.05	0.05	0.011	0.012	0.01	0.015	0.008	0.006	0.005	0.003	Final Crack Length After Surface Finish Was Applied (in)
5	Crack length	—	0.202	—	—	—	—	—	—	—	—	—	—	0.218
6	Crack length	—	—	0.153	—	—	0.172	0.157	—	—	—	0.12	—	0.037
7	Crack length	—	—	0.29	0.278	—	0.275	0.257	0.175	0.127	0.098	-	—	0.098
8	Crack length	—	—	0.196	0.195	—	0.157	0.15	—	—	—	0.115	0.102	0.098
9	Crack length	—	—	0.247	0.237	—	0.224	0.171	—	0.092	—	—	—	0.047
10	Crack length	—	—	0.203	—	—	—	—	—	—	—	—	—	0.225

Table 6. Magnesium grinding data.

Bar No.	Machine Removed	0.015	0.015	0.005	0.006	Final Crack Length After Surface Finish Was Applied (in)
1	Crack length	0.182	0.165	0.15	0.1	0.10
2	Crack length	—	0.199	—	—	0.199
3	Crack length	—	0.202	—	—	0.202
6	Crack length	0.198	0.1	—	—	0.100
7	Crack length	—	—	—	—	0.025
8	Crack length	—	—	—	—	0.025

Table 7. Titanium grinding data.

Bar No.	Machine Removed	0.015	0.005	0.01	0.007	0.01	0.015	0.03	0.04	0.03	0.03	0.01	0.01	0.02	0.01	0.007	Final Crack Length After Surface Finish Was Applied (in)
3	Actual removed Thickness	—	—	0.0105	0.0035	0.005	0.007	0.0115	0.0155	0.012	0.015	—	—	—	—	—	0.200
	Crack length	0.222	0.217	0.23	0.245	0.24	0.24	0.23	0.2	0.225	0.2	—	—	—	—	—	
4	Actual removed Thickness	—	0.465	0.0025	0.0045	0.006	0.004	0.0135	0.016	0.0125	0.015	0.005	—	0.013	0.0055	0.0055	0.028
	Crack length	0.27	0.245	0.3	0.265	0.26	0.265	0.265	0.225	0.24	0.21	0.382	—	0.15	0.13	0.098	
6	Actual Removed Thickness	—	—	0.007	0.004	0.005	0.005	0.0135	0.016	0.0115	0.0155	0.0065	—	0.012	0.0055	0.0055	0.102
	Crack length	0.4695	—	0.4625	0.454	0.449	0.444	0.4305	0.403	0.419	0.3875	0.381	—	0.369	0.3635	0.358	
7	Actual removed Thickness	—	—	0.0005	0.0035	0.0055	0.0055	0.0125	0.017	0.012	—	—	—	0.016	0.0235	—	0.030
	Crack length	0.25	0.23	0.237	0.265	0.26	0.245	0.24	0.195	0.238	0.21	0.197	—	0.19	0.09	—	
8	Actual removed Thickness	—	—	0.005	0.004	0.005	0.006	0.011	0.016	0.0135	0.014	0.0055	—	0.013	0.0055	—	0.102
	Crack length	0.245	0.265	0.26	0.265	0.26	0.26	0.265	0.235	0.26	0.215	0.196	—	0.15	0.102	—	
9	Actual removed Thickness	—	—	0.004	0.0045	0.005	0.006	0.0125	0.0185	0.011	0.014	0.0055	—	—	—	—	0.202
	Crack length	0.25	0.219	0.262	0.29	0.285	0.272	0.27	0.26	0.285	0.24	0.215	0.202	—	—	—	

Table 8. Steel grinding data.

Bar No.	Machine Removed	0.1	0.2	0.025	0.02	0.03	0.02	0.02	0.005	Final Crack Length After Surface Finish Was Applied (in)
1	Actual removed	0.0137	0.0128	0.0195	—	0.3534	0.0134	—	—	0.025
	Thickness	0.4148	0.402	0.3825	—	0.3534	0.34	—	—	—
	Crack length	0.25	0.215	0.2	—	0.13	0.025	—	—	—
2	Actual removed	0.0129	0.0139	0.0192	0.0133	0.0183	0.0099	0.011	0.003	0.100
	Thickness	0.4141	0.4002	0.381	0.3677	0.3494	0.3395	0.3285	0.3255	—
	Crack length	0.3	0.27	0.25	0.225	0.19	0.15	0.12	0.1	—
3	Actual removed	0.0131	0.0144	0.0205	0.003	0.0218	0.0196	—	—	0.030
	Thickness	0.4139	0.3995	0.379	0.376	0.3542	0.3346	—	—	—
	Crack length	0.25	0.25	0.225	0.195	0.155	0.03	—	—	—
4	Actual removed	0.0137	0.0153	0.0207	—	0.0243	—	—	—	0.090
	Thickness	0.4133	0.398	0.3773	—	0.353	—	—	—	—
	Crack length	0.25	0.215	0.19	—	0.09	—	—	—	—
5	Actual removed	0.0145	0.0169	0.0211	—	—	—	—	—	0.185
	Thickness	0.413	0.3961	0.375	—	—	—	—	—	—
	Crack length	0.25	0.215	0.195	—	—	—	—	—	—
6	Actual removed	0.0144	0.0177	—	—	—	—	—	—	0.185
	Thickness	0.4131	0.3954	—	—	—	—	—	—	—
	Crack length	0.225	0.2	—	—	—	—	—	—	—

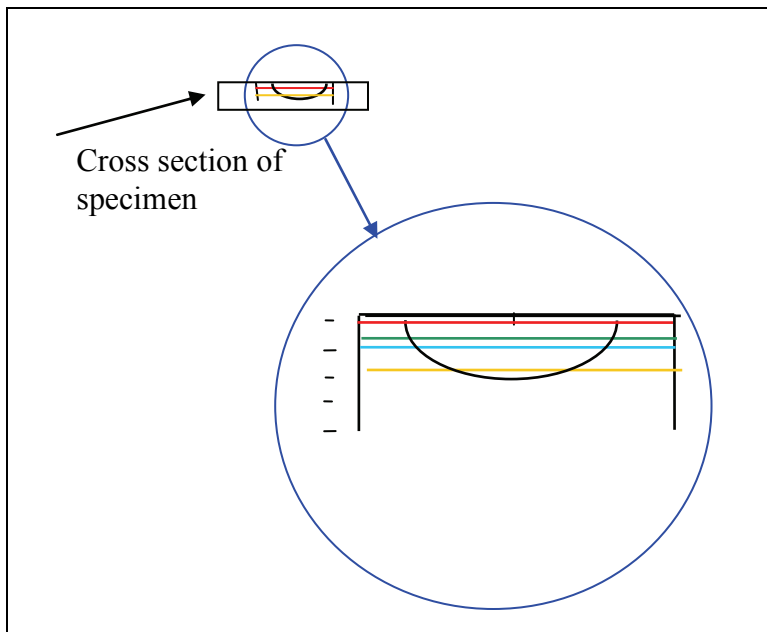


Figure 2. Schematic of the cross section of a typical fatigue-cracked test specimen depicting the incremental removal of material from the top surface and its corresponding effect on crack-length reduction.

#### **4.4 Light Optical Photometer**

A certified inspector typically interprets indications. Since there can be considerable variation in interpretation of an indication from inspector to inspector, a light photometer was employed to detect the brightness of the indications and to measure any effect of the paint. This makes the FPI results considerably more quantitative than qualitative. There still exists some qualitative interpretation, however, as the photometer can not easily distinguish an intense, sharp, clear indication from a more intense but less sharp indication, typically referred to as “fuzzy.” Indications are fuzzy when excess penetrant bleeds out from a crack. This occurs for several reasons, which include residues left behind in and around the crack, cleaner left behind from inadequate rinsing (or long evaporation times for solvent use), and water left behind from rinsing and inadequate drying. The equipment utilized for this program was the Photo Research, Model UBD, PR-1500 Spectra Spotmeter, Photomultiplier-Tube Optical Photometer. The data was acquired in foot-lamberts (FL), equivalent to 0.3183 candles/ft<sup>2</sup>. Satisfactory results are obtained from readings with a large difference between the background fluorescence value and the indication fluorescence value, coupled with sharp distinct crack indications. Background values will vary slightly based upon available background light (if it is not completely eliminated).

---

#### **5. Materials Pretreatment**

The Ti-6-4 specimens were painted bare, but the other three materials had pretreatments applied as on typical aviation components manufactured from these materials. The steel specimens were cadmium coated IAW-SAE-AMS-QQ-P-416, Type II, Class II. The magnesium specimens were coated with Tagnite 8200 coating at a thickness of 0.32 mil. The aluminum specimens were anodized IAW MIL-A-8625. Following their respective pretreatment, the specimens underwent NDI to record baseline measurements for the crack sizes utilized.

---

#### **6. FPI/MPI and Light Measurements**

The penetrant materials included Sherwin water-washable HM-607 (sensitivity level 3) penetrant and Zyglow ZP-4B developer. The MPI was performed in a full wave direct current wet bath booth using 14A Magnaflux particulate with a particle concentration of 0.35 in a standard centerfuge. The flux density was set to 58–60 G. The light intensity for the inspection was set at 1400 candle-W<sup>2</sup> at 18 in. Post inspection processing involved degaussing and a solvent wash. FPI was performed in accordance with ASTM-E-1417 (7) and MPI in accordance with ASTM-E-1444 (8).

Brightness measurements were taken with a PR-1500 Spectra\* spotmeter optical photometer. The measurement of light intensity has units of FL. For consistency in the light measurements (the photometer is very sensitive), the unit was calibrated before each use. With the blacklight placed next to the photometer, the center of the blacklight beam was focused on the platform. Using a Spectroline† hand held digital radiometer, the light beam was adjusted until the radiometer gave a reading of  $10,500 \mu\text{W}/\text{cm}^2$  ( $\pm 500$ ) with the spotmeter focused on the radiometer panel. The bars were placed on the platform one at a time, and the lens was focused on the crack. The spot was placed on one of the crack ends, and the reading was recorded. The spot was then placed on an area adjacent to the crack end, and a background measurement was taken. After all the measurements were taken the cracks were digitally recorded.

Once the FPI had been performed, the bars were cleaned to prevent the penetrant from drying in the crack. It is very difficult to remove dried penetrant from a crack. An ARL standard cleaning procedure was followed. First, the bars (Al, Mg, Ti) were placed in sonic tank with an NSK (Nakanishi, Inc.) cleaner (a blend of dentured alcohol and methylene chloride) for 5 min. Then they were placed in a drying oven for 5 min. Next, they were taken out of the oven and placed in another sonic tank filled with dimethyl formamide for 5 min. Then, they were rinsed with warm tap water and put back in the oven to dry. Finally, they were placed in a sonic tank filled with acetone for at least 1 hr. This very thorough procedure was not always necessary and was altered when conditions warranted. As stated previously, the steel bars were cleaned in a solvent wash after MPI.

---

## 7. Painting

---

The bars were painted to a dry film thickness of 1–1.5 mil with an epoxy primer (MIL-P-23377). New CARC was then applied to a dry film thickness of 2–2.5 mil for the topcoat (MIL-C-64159). After the paint was applied, the bars were air dried for 1 week and baked at 150 °F for 1 week. Once the coating system had been applied, FPI/MPI was performed on the bars, and brightness measurements of the cracks were taken.

---

## 8. Crack Extension After Painting

---

One bar of each crack length for each material was extended. The same set up as when the cracks were originally extended was used, except a three-point bend fixture was used instead of a

---

\*PR-1500 Spectra is a registered trademark of Photo Research, Inc.

†Spectroline is a registered trademark of Spectronics Corporation.

four-point bend fixture. Three-point bending calculations were tabulated for the bars showing the estimated required loads to extend each crack 0.5 in. After the extension, the cracks were inspected via FPI, and light measurements with the spotmeter were recorded. It is important to note that extending cracks with paint on them is much more difficult than extending bare bars. The paint masked the crack's true length and made it difficult to see the crack during the extension process. The painted-bar crack extension data can be observed in table 9.

---

## **9. Plastic Media Blasting**

---

The aluminum, titanium, and magnesium bars were plastic media blasted (PMB) with Type V acrylic (thermal) plastic media IAW MIL-P-85891 (9). The original test matrix blasts the primer first and blasts the substrate after FPI. Even after attempting PMB on numerous actual aviation components and adjusting parameters such as air pressure, angle, and distance, blasting to the primer on the specimens could not be accomplished. The plastic media either removed nothing, or it removed the top coat and primer at the same time, which doesn't allow for the separation of the two coating layers. The bonding between the primer and the topcoat proved to be much stronger than that of the actual components. Consequently, only one FPI iteration could be performed on the bars, and no differentiation could be made between the top coat and primer.

The various types of plastic media utilized in PMB must be discussed. PMB facilities typically use a single type of plastic media, which they use for all of their PMB work. Most U.S. Department of Defense facilities use either Type II or Type V media. Type V media is not as hard as Type II media and is gentler on substrates. Type V media is more commonly used on aircraft. In some cases, Type II might be hard enough to deform the surface of a soft metal and smear material over a crack. Type II is recommended for steel-only surfaces.

ARL has evaluated PMB prior to FPI cleaning. The study ARL performed involved Type II media, which demonstrated good performance for harder metals. For this project, Type V (softer and gentler than Type II) was used. It was found that Type V can be detrimental to FPI and can mask the presence of cracks, especially in softer materials. When striking a surface, the softer plastic is able to deform and wedge itself into the crack. This effectively masks the crack and blocks any penetrant from getting in. The cracks in the aluminum and magnesium samples could easily be seen under the microscope and, in some cases, even without the aid of magnification; however, no indications were revealed during FPI. Titanium is much harder than aluminum and magnesium and so PMB did not appear to affect the titanium as much as the other samples. The titanium crack is also much narrower than the other two metals, which makes it more difficult for the plastic media particles to wedge into the crack. PMB also didn't seem to affect the smaller cracks as much as the larger ones—even the 0.025-in cracks of the aluminum and magnesium showed indications during FPI after PMB. This could also be due to the crack width being larger at longer crack lengths.

Table 9. Data after paint crack extension.

Bar No., Length	Length Before Extension (in)	Length After Extension (in)	Cycling Load (lb)	(±) (lb)	Total Cycles	Notes
Al no. 10, 0.2	0.2	0.26	476	390	10,000	No crack
			476	390	17,201	Complete
Al no. 8, 0.1	0.1		432	350	10,000	No visible cracking of paint, placed marker dots to monitor growth
			432	350	50,000	No visible cracking
			432	350	145,103	No crack observed with FPI or microscopic inspection
			486	398	180,000	Changed to 10% reduction, crack can be seen, est. at 0.1 in, marked ends and attempt to extend
	0.15		486	398	205,002	Complete
Al no. 9, 0.025	0.03		429	351	40,000	No visible crack
		0.083	429	351	175,001	Complete
Ti no. 9, 0.2	0.2	0.275	2409	1971	989	Crack extended, complete
Ti no. 6, 0.1	0.1	0.15	1645	1346	3800	Crack extended and done, used parameters for bar no. 8
Ti no. 7, 0.025	0.025	0.3	1440	1178	14,414	Crack extended longer than 50 mil limit, done
Mg no. 3, 0.2	0.2	0.201	242	198	6000	Crack visible, no growth observed
	0.2	0.202	242	198	20,000	Crack visible, no growth observed
	0.2	0.25	242	198	59,998	Complete
Mg no. 6, 0.1	0.1	0.1	219	179	20,000	No visible crack
		0.125	219	179	49,995	Crack visible
		0.13	219	179	61,003	Crack visible
		0.15	219	179	75,002	Complete
Mg no. 7, 0.025	0.025		225	184	40,002	No visible crack
		0.052	225	184	100,001	Crack visible, needs more extension
		0.25	2413	1947	3063	Complete
St no. 6, 0.2	0.185		1655	1354	7064	Complete
St no. 2, 0.1	0.1	0.145	1358	1111	21,349	No visible crack
St no. 3, 0.025	0.03	0.075	1358	1111	50,501	Complete

Notes: All lengths after crack extension were estimated using a stereo microscope.

Loop shaping parameters:

Prop = -0.449.

Int = 3.09

Deriv = 0.947.

Both the extended and unextended bars were stripped with PMB. On the bars with crack extensions, some extension of the cracks could be observed through the paint during and after the extension process. However, when the paint was stripped off via PMB, the cracks were not detectable by FPI. This indicated that the PMB was directly responsible for the decline in performance.

---

## **10. Chemical Removal of Paint**

---

After PMB, the bars were placed in Brulin Industrial Safety Strip 5896B hot tank paint stripper and allowed to soak for ~24 hr. They were then removed and cleaned with solvent so FPI could be performed to see if there was any change. As indicated in the previous section, the plastic media was getting wedged into the magnesium and aluminum cracks, and the FPI was yielding affected indications. After soaking in paint stripper for 24 hr, there still were no visible indications. This demonstrated that the material within the crack, the Type V plastic media, was not dissolved or displaced by the stripper. To refresh the indications, the cracks needed to be mechanically opened. This involved placing the specimens back on the mechanical test stand and loading them to a deflection of about 1/8 in. After doing this, all bars again revealed indications of the cracks during subsequent FPI. When loading, the bars were first placed with the crack face in compression and then turned over with the crack face placed in tension. This needed to be completed on the extended as well as the unextended samples.

---

## **11. Results**

---

### **11.1 Aluminum**

The brightness measurements for aluminum can be found in table 10. The greatest intensity measurements came from the initial bare baseline condition. This condition also generally yielded the highest difference between the crack intensity and the background intensity. Figure 3 shows an optical photograph of bare aluminum crack no. 7. This is typical of the cracks formed in the aluminum material used for this study. The typical results for the FPI indications in the baseline condition are visually represented in figure 4. Figure 5 depicts the typical location of the spotmeter in relation to the cracks. After the bars were anodized, the intensities and the difference between the crack and background intensities were reduced. Figure 6 shows specimen no. 7 with typical visual FPI results after anodizing. No brightness measurements were taken after the coating system had been applied to the bars because no indications could be observed. Figure 7 shows specimen no. 7 with typical FPI visual results. No crack can be observed and

Table 10. Aluminum spotmeter readings.

Specimen Identification	Spotmeter Indication Measurement	Spotmeter Background Measurement	Difference	After Pretreatment	After Pretreatment Background	Difference	After Painting Measurement	After Painting Background	Difference
Al no. 6 – 0.025	$1.68 \times 10^1$	$1.92 \times 10^{-1}$	16.608	$1.50 \times 10^0$	$4.59 \times 10^{-1}$	1.041	Not visible	Not visible	—
Al no. 7 – 0.1	$10.30 \times 10^1$	$1.54 \times 10^{-1}$	102.85	$6.70 \times 10^0$	$6.57 \times 10^{-1}$	6.043	Not visible	Not visible	—
Al no. 5 – 0.2	$3.64 \times 10^1$	$1.32 \times 10^{-1}$	36.268	$6.05 \times 10^1$	$2.55 \times 10^{-1}$	60.245	Not visible	Not visible	—
Al no. 9 – 0.025	$1.29 \times 10^1$	$1.27 \times 10^{-1}$	12.773	$3.96 \times 10^0$	$6.95 \times 10^{-1}$	3.265	—	—	—
Al no. 8 – 0.1	$4.79 \times 10^1$	$1.23 \times 10^{-1}$	49.577	$3.52 \times 10^0$	$6.12 \times 10^{-1}$	2.908	—	—	—
Al no. 10 – 0.2	$11.42 \times 10^1$	$1.93 \times 10^{-1}$	114.01	$2.98 \times 10^1$	$6.33 \times 10^{-1}$	29.167	—	—	—
Specimen Identification	After Plastic Media Blast Measurement	After Plastic Media Blast Background	Difference	After Paint Stripper Measurement	After Paint Stripper Background	Difference	After Mechanical Flexing Measurement	After Mechanical Flexing Background	Difference
Al no. 6 – 0.025	Not visible	Not visible	—	Not visible	Not visible	—	$2.34 \times 10^1$	$2.22 \times 10^1$	1.2
Al no. 7 – 0.1	Not visible	Not visible	—	Not visible	Not visible	—	$2.82 \times 10^1$	$1.20 \times 10^1$	16.2
Al no. 5 – 0.2	Not visible	Not visible	—	Not visible	Not visible	—	$10.48 \times 10^1$	$1.15 \times 10^1$	93.3
Al no. 9 – 0.025	—	—	—	—	—	—	—	—	—
Al no. 8 – 0.1	—	—	—	—	—	—	—	—	—
Al no. 10 – 0.2	—	—	—	—	—	—	—	—	—
Specimen Identification	After Crack Extension Background	After Crack Extension Background	Difference	After Extension PMB Background	After Extension and Mechanical Flexing Measurement	Difference	After Extension and Chemical Stripper Processing Background	After Extension and Chemical Stripper Processing Background	Difference
Al no. 6 – 0.025	—	—	—	—	—	—	—	—	—
Al no. 7 – 0.1	—	—	—	—	—	—	—	—	—
Al no. 5 – 0.2	—	—	—	—	—	—	—	—	—
Al no. 9 – 0.025	$2.54 \times 10^1$	$1.49 \times 10^1$	10.5	Not visible	$14.83 \times 10^0$	$0.43 \times 10^0$	$18.56 \times 10^0$	$2.28 \times 10^0$	16.28
Al no. 8 – 0.1	$1.53 \times 10^1$	$0.77 \times 10^1$	7.6	Not visible	$15.7 \times 10^0$	$0.25 \times 10^0$	$22.32 \times 10^0$	$2.66 \times 10^0$	19.66
Al no. 10 – 0.2	$2.13 \times 10^1$	$1.87 \times 10^1$	2.6	Not visible	$8.89 \times 10^0$	$0.28 \times 10^0$	$14.90 \times 10^1$	$3.00 \times 10^1$	119

Notes: All measurements were obtained with FPI.

All measurements are in units of foot-lamberts.

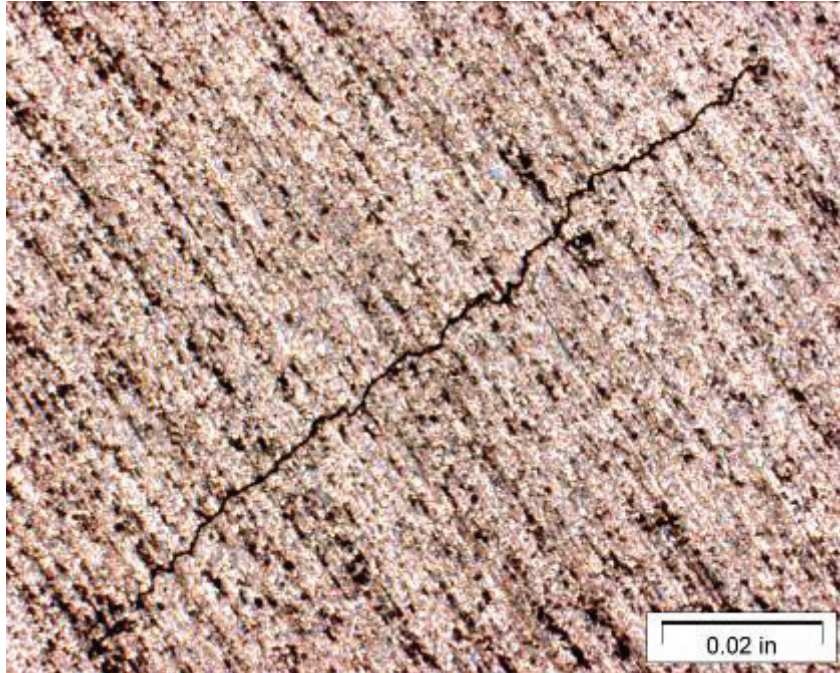


Figure 3. Al bar no. 7 after initiation and extension (shows crack at its final length).

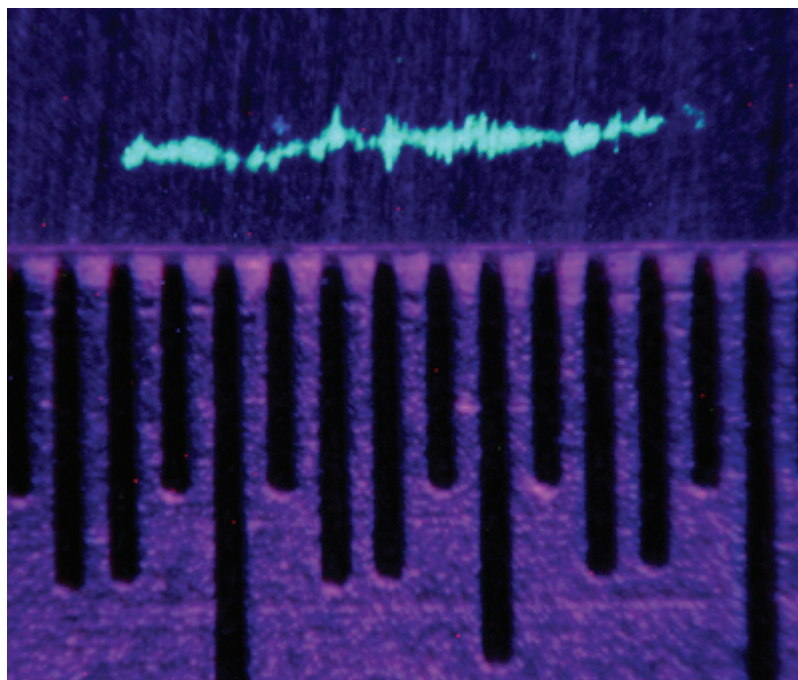


Figure 4. FPI of Al bar no. 7 after initiation and extension.

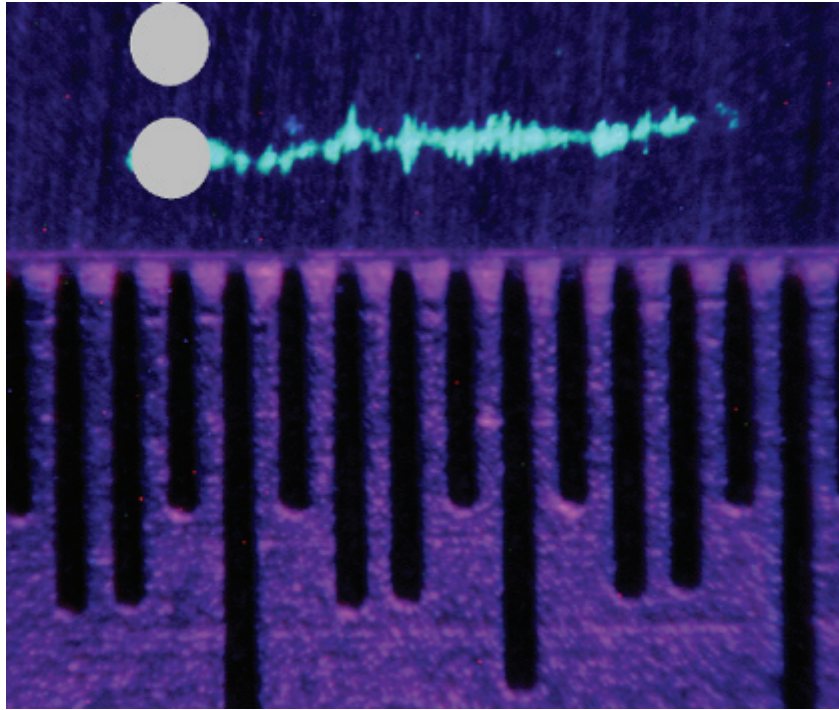


Figure 5. Al bar no. 7 illustrating the manner in which the brightness measurements were acquired. The top dot represents the area the spotmeter was focused for the background measurement, and the bottom dot represents the area from which the crack measurement was acquired.

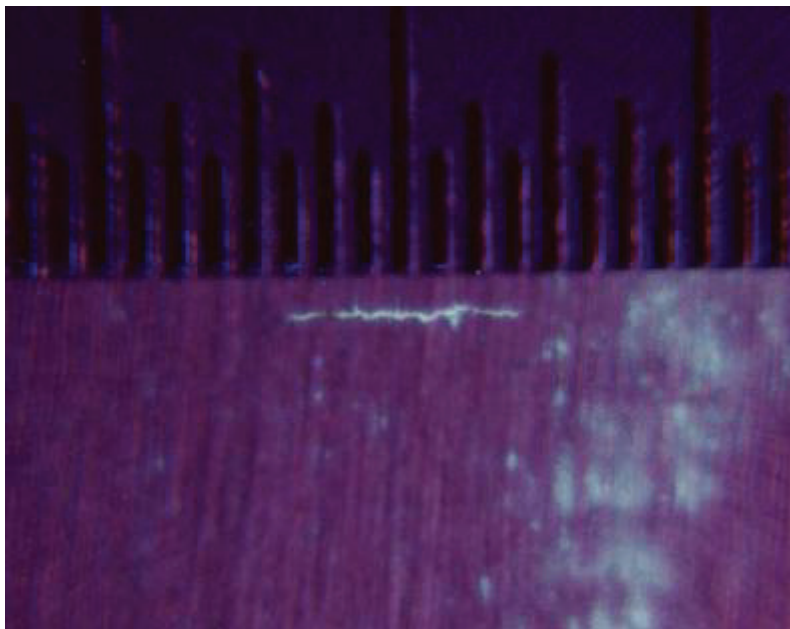


Figure 6. FPI of Al bar no. 7 crack after anodizing.

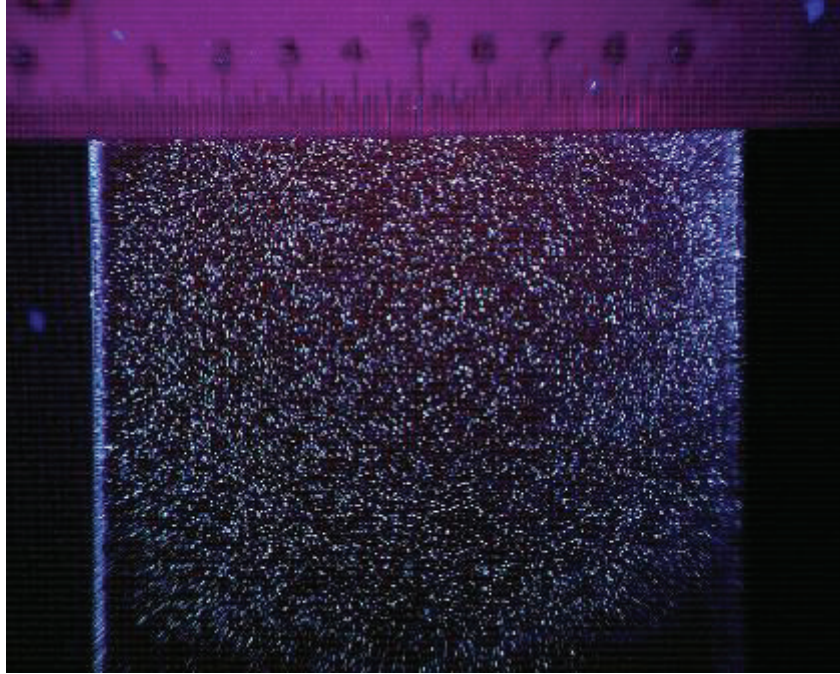


Figure 7. FPI of Al bar no. 7 crack after painting.

extreme background fluorescence from the paint absorbing the penetrant is evident. No brightness measurements were taken after PMB because zero indications were observed during FPI. The typical results are shown for specimen no. 7 (figure 8). Note how the crack has no visible infiltration of the penetrant. After the bar was processed in paint stripper and mechanically flexed, the crack was again apparent (figure 9). The brightness measurements taken for bars 8, 9, and 10 after chemical paint stripper processing were recorded after the cracks were flexed on the mechanical testing machine. Before they were flexed, no indications were visible. The resulting indications for cracks 8, 9, and 10 after this process can be observed in figure 10. Note again the extreme background fluorescence, resulting in low contrast between the background and the indications.

## 11.2 Titanium

Figure 11 presents an SEM micrograph of a typical bare titanium crack after initial extension. The corresponding brightness measurements for titanium can be found in table 11. The initial baseline measurements yielded the highest values of any category, and the difference between the crack intensity and the background intensity for this group yielded the highest contrast. The typical resultant FPI is visual depicted in figure 12. Figure 13 shows the typical areas where the light measurements were recorded. No indications were observed after the paint was applied, so no readings were recorded. Figure 14 presents the typical visual FPI results after paint was applied. The brightness measurements taken after the painted bars were extended were much

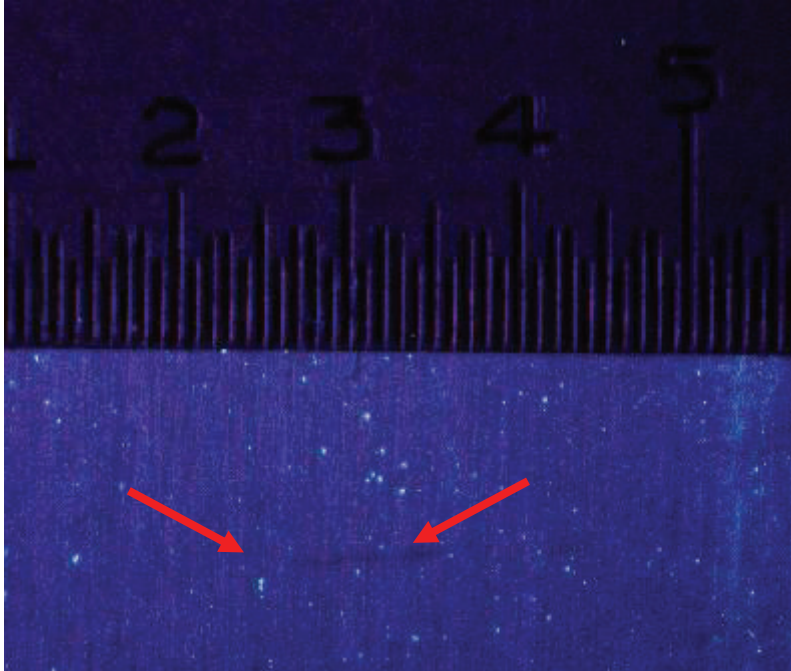


Figure 8. FPI of Al bar no. 7 after PMB. The crack can be observed visually, but no indication can be observed.

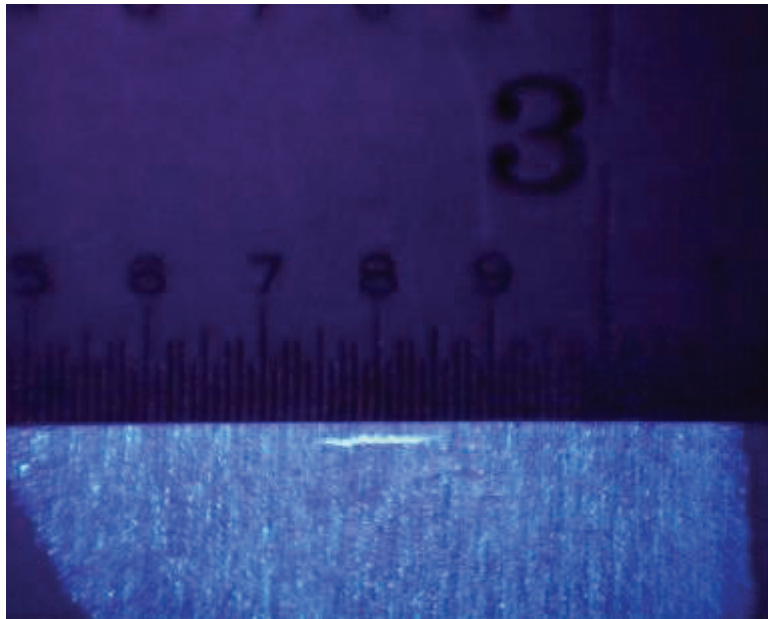


Figure 9. FPI of Al bar no. 7 performed after the bar had been processed in paint stripper and after the bar had been mechanically flexed.

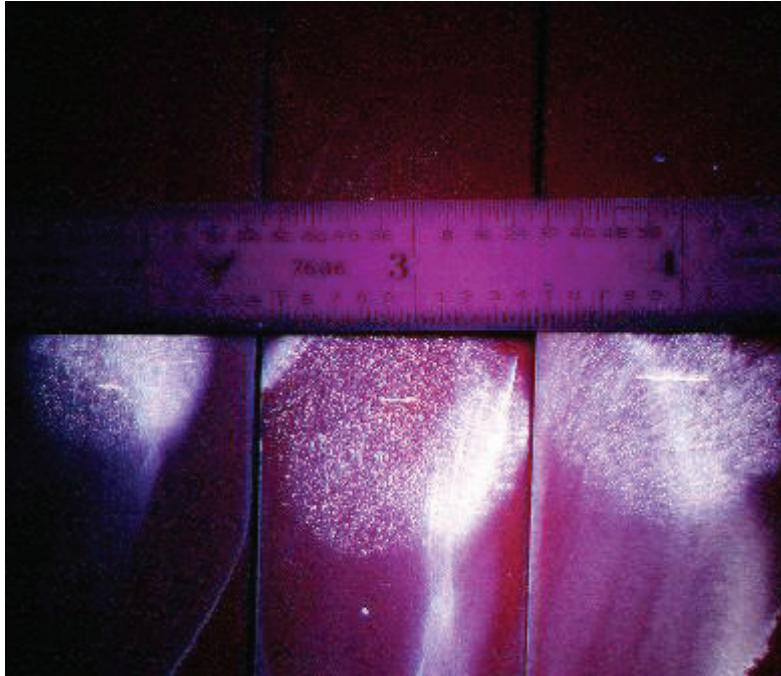


Figure 10. FPI of Al bar nos. 8, 9, and 10—the bars with cracks extended  $\sim 0.050$  in after painting—performed after the bars had been painted and the cracks mechanically flexed.

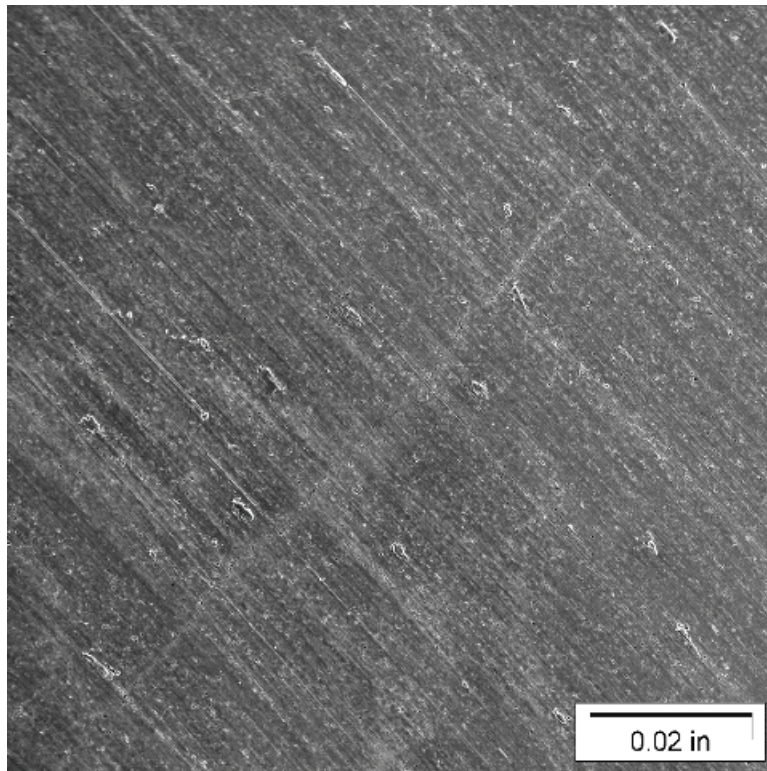


Figure 11. Titanium bar no. 6—0.1-in crack after initial crack extension.

Table 11. Titanium spotmeter readings.

Specimen Identification	Initial Crack Measurement	Initial Crack Background Measurement	Difference	After Painting Measurement	After Painting Background	Difference	After Plastic Media Measurement	After Plastic Media Background	Difference
Ti no. 4 - 0.025	$3.30 \times 10^1$	$1.25 \times 10^{-1}$	32.875	Not visible	Not measured	—	Not visible	Not measured	—
Ti no. 8 - 0.1	$6.94 \times 10^1$	$1.57 \times 10^{-1}$	69.243	Not visible	Not measured	—	$2.10 \times 10^0$	$0.7 \times 10^{-1}$	2.03
Ti no. 3 - 0.2	$7.68 \times 10^1$	$1.06 \times 10^{-1}$	76.694	Not visible	Not measured	—	$8.45 \times 10^0$	$0.6 \times 10^{-1}$	8.38
Ti no. 7 - 0.025	$6.20 \times 10^1$	$1.50 \times 10^{-1}$	61.85	—	—	—	—	—	—
Ti no. 6 - 0.1	$10.16 \times 10^1$	$1.66 \times 10^{-1}$	101.434	—	—	—	—	—	—
Ti no. 9 - 0.2	$7.38 \times 10^1$	$1.48 \times 10^{-1}$	73.652	—	—	—	—	—	—
Specimen Identification	After Paint Stripper Processing Measurement	After Paint Stripper Processing Background	Difference	After Flexing Measurement	After Flexing Background	Difference	After Crack Extension Measurement	After Crack Extension Background	Difference
Ti no. 4 - 0.025	Not visible	Not measured	—	$1.36 \times 10^1$	$0.27 \times 10^0$	13.573	—	—	—
Ti no. 8 - 0.1	$0.46 \times 10^0$	$0.07 \times 10^0$	0.39	$6.01 \times 10^1$	$0.09 \times 10^0$	60.01	—	—	—
Ti no. 3 - 0.2	$1.95 \times 10^0$	$0.06 \times 10^0$	1.89	$2.46 \times 10^1$	$0.03 \times 10^0$	24.57	—	—	—
Ti no. 7 - 0.025	—	—	—	—	—	—	$11.44 \times 10^0$	$2.29 \times 10^0$	9.15
Ti no. 6 - 0.1	—	—	—	—	—	—	$8.79 \times 10^0$	$2.62 \times 10^0$	6.17
Ti no. 9 - 0.2	—	—	—	—	—	—	$15.47 \times 10^0$	$3.05 \times 10^0$	12.42
Specimen Identification	After Extension PMB Measurement	After Extension PMB Background	Difference	After Extension, PMB, and Mechanical Flexing Measurement	After Extension, PMB, and Mechanical Flexing Background	Difference	After Extension, PMB, Flexing, and Chem Stripper Measurement	After Extension, PMB, Flexing, and Chem Stripper Background	Difference
Ti no. 4 - 0.025	—	—	—	—	—	—	—	—	—
Ti no. 8 - 0.1	—	—	—	—	—	—	—	—	—
Ti no. 3 - 0.2	—	—	—	—	—	—	—	—	—
Ti no. 7 - 0.025	Very faint	Not measured	—	$6.56 \times 10^0$	$0.70 \times 10^{-1}$	6.49	$8.48 \times 10^0$	$0.09 \times 10^0$	8.39
Ti no. 6 - 0.1	Not visible	Not measured	—	$2.26 \times 10^0$	$0.83 \times 10^{-1}$	2.177	$9.89 \times 10^0$	$0.04 \times 10^0$	9.85
Ti no. 9 - 0.2	Very faint	Not measured	—	$2.08 \times 10^1$	$0.80 \times 10^{-1}$	20.72	$26.31 \times 10^0$	$0.06 \times 10^0$	26.25

Notes: All measurements were obtained with FPI  
All measurements are in units of foot-lamberts.

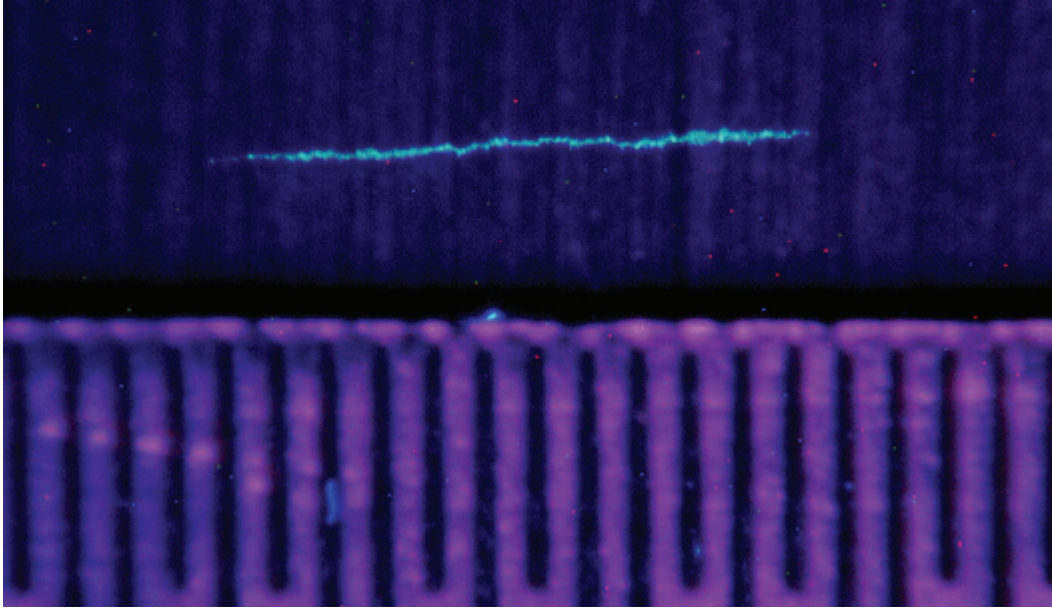


Figure 12. FPI of titanium bar no. 6—0.1-in crack after initial crack extension.

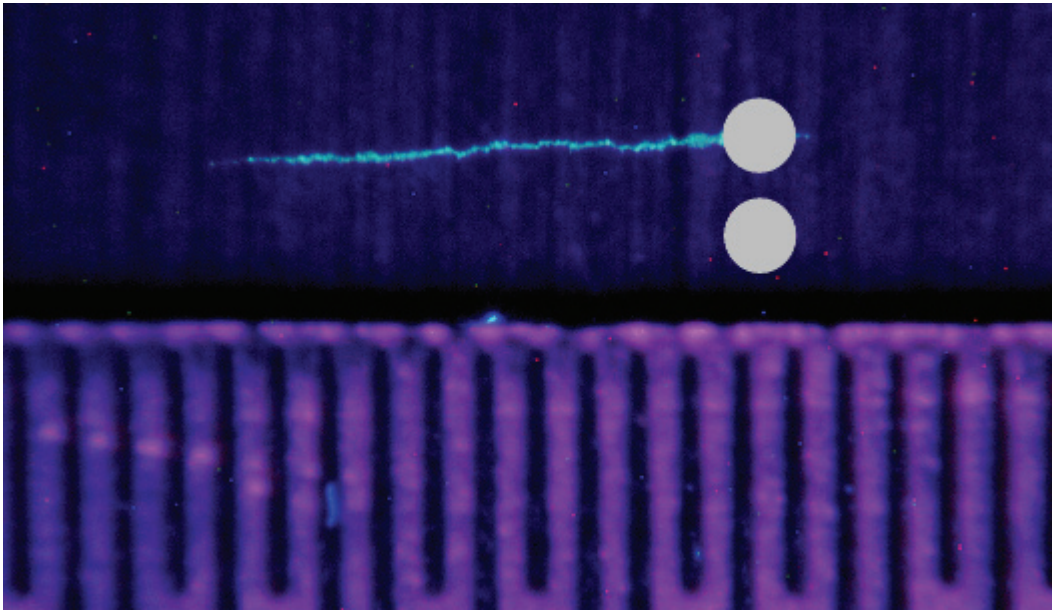


Figure 13. FPI of titanium bar no. 6 showing areas where brightness measurements were taken. The top spot is the brightness of the crack, and the bottom spot (below the crack) is where the background reading was taken.

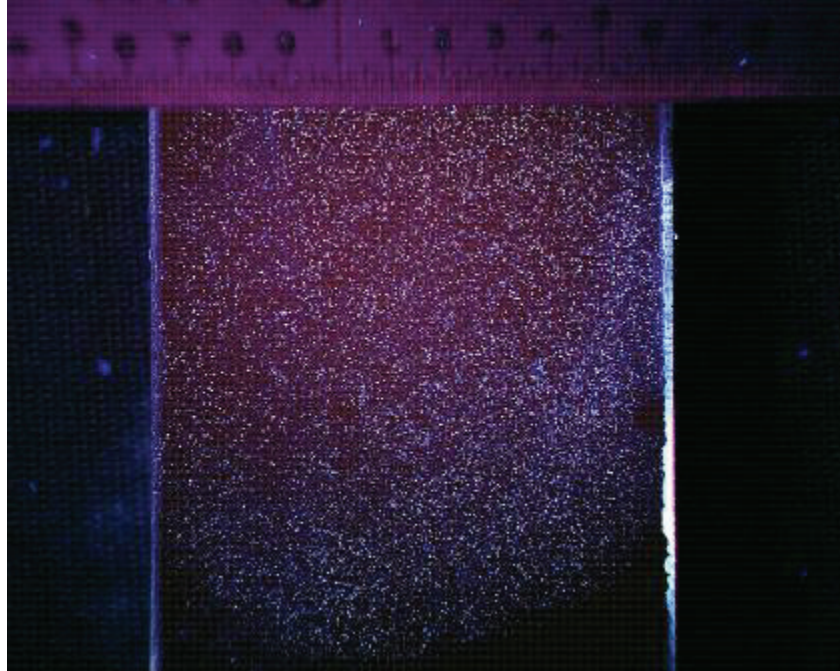


Figure 14. FPI of titanium bar no. 6 after painting.

dimmer than the initial measurements. The difference between the crack measurement and the background measurement was also greatly reduced. During FPI, only faint indications could be visually observed (figure 15). Titanium was the only material out of the three that demonstrated visible indications after PMB. Figure 16 shows an optical micrograph depicting the crack in titanium bar no. 6 after PMB. The indications were faint compared to the baseline measurements, and in some cases, portions of the crack length were masked completely. Ultimately, the titanium bar cracks required mechanical flexing on the mechanical test frame (like the aluminum and magnesium). Figure 17 shows the resultant visual FPI of titanium bar no. 6 after PMB and mechanical flexing. After chemical-stripper processing, the results were similar to those after the crack extension of  $\sim 0.05$  in. These results are depicted in figure 18.

### 11.3 Magnesium

The magnesium bar brightness measurements can be found in table 12. An optical micrograph of the bare magnesium crack no. 2 is shown in figure 19. This is typical of the cracks in the magnesium material utilized in this work. The typical results for the FPI indications in the baseline condition are shown in figure 20. Figure 21 depicts the typical location of the spotmeter in relation to the cracks. The Tagnite pretreatment process tended to increase dramatically the brightness of the indications. Figure 22 presents the visual FPI results on bar no. 2 after Tagnite pretreatment. This pretreatment also absorbed a considerable amount of penetrant, which resulted in high background brightness values. This could be due to the characteristics of the Tagnite in the vicinity of a crack. The pretreatment was visibly nonuniform in this area, which

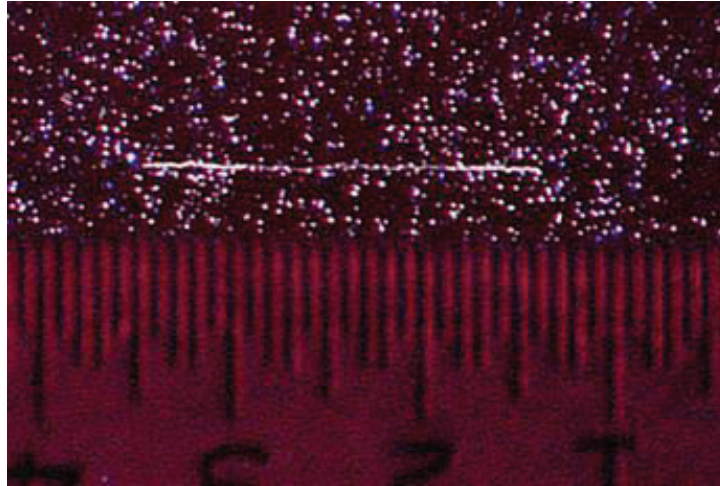


Figure 15. FPI of titanium bar no. 6 after the painted bar had been extended by 0.5 in.

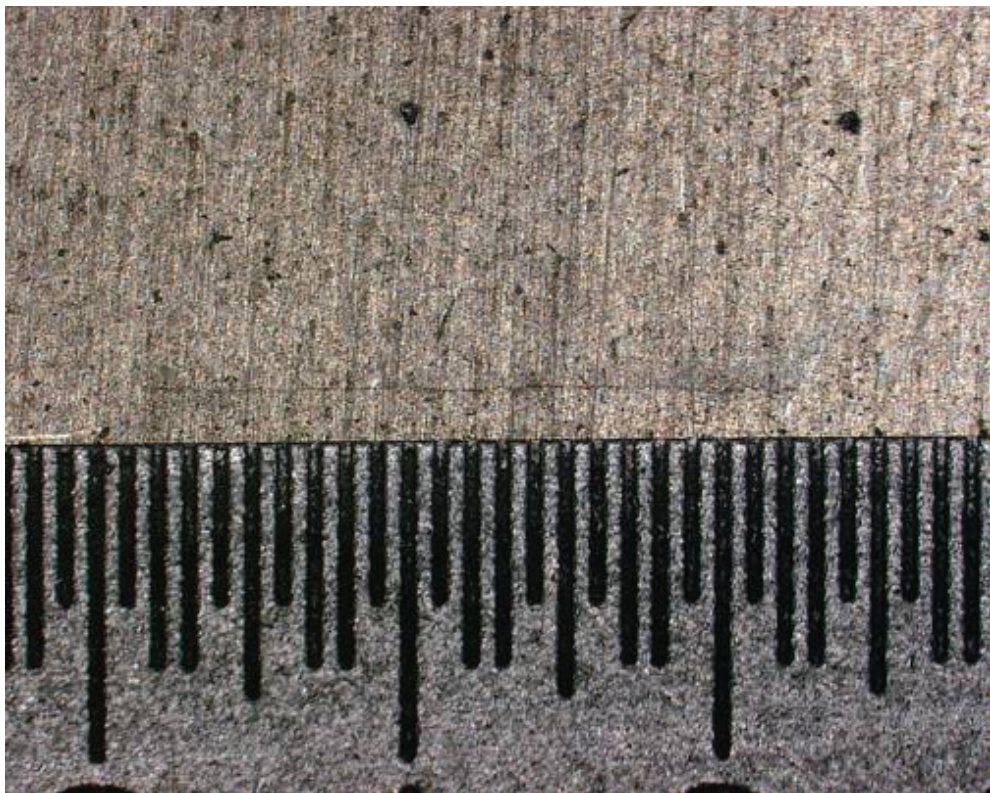


Figure 16. Optical micrograph of titanium bar no. 6 showing the extended crack after PMB.



Figure 17. FPI micrograph of titanium bar no. 6 after PMB and mechanical flexing. Initial FPI produced no visible indication after PMB.

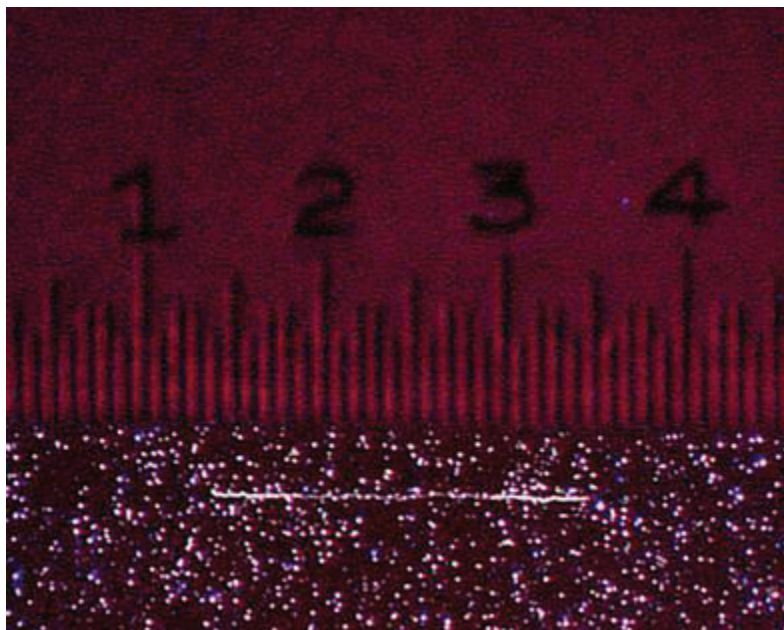


Figure 18. FPI micrograph of titanium bar no. 6 after PMB and chemical-stripper processing. The results are similar to those after painting and crack extension.

Table 12. Magnesium spotmeter measurement.

Specimen Identification Crack Length	Spotmeter Indication Measurement	Spotmeter Background Measurement	Difference	After Tagnite Pretreatment	After Tagnite Pretreatment Background	Difference	After Painting Measurement	After Painting Background	Difference
Mg no. 8 - 0.025	$1.35 \times 10^1$	$1.50 \times 10^{-1}$	13.35	$1.57 \times 10^1$	$3.97 \times 10^0$	11.73	Not visible	Not measured	—
Mg no. 1 - 0.1	$2.55 \times 10^1$	$1.66 \times 10^{-1}$	25.334	$2.80 \times 10^2$	$6.65 \times 10^0$	273.35	Not visible	Not measured	—
Mg no. 2 - 0.2	$8.49 \times 10^1$	$1.06 \times 10^{-1}$	84.794	$9.80 \times 10^2$	$3.66 \times 10^0$	976.34	Not visible	Not measured	—
Mg no. 7 - 0.025	$3.22 \times 10^1$	$1.25 \times 10^{-1}$	3.095	$1.12 \times 10^2$	$8.47 \times 10^0$	103.53	—	—	—
Mg no. 6 - 0.1	$2.84 \times 10^1$	$1.57 \times 10^{-1}$	28.243	$3.59 \times 10^2$	$2.47 \times 10^0$	356.53	—	—	—
Mg no. 3 - 0.2	$6.98 \times 10^1$	$1.48 \times 10^{-1}$	69.652	$4.70 \times 10^2$	$1.03 \times 10^1$	459.7	—	—	—
Specimen Identification Crack Length	After Plastic Media Measurement	After Plastic Media Background	Difference	After PMB and Paint Stripper Processing	After PMB and Paint Stripper Processing Background	Difference	After PMB, Chem Stripper and Flexing Measurement	After PMB, Chem Stripper and Flexing Background	Difference
Mg no. 8 - 0.025	Not visible	Not measured	—	Not visible	Not measured	—	Not visible	$3.96 \times 10^1$	—
Mg no. 1 - 0.1	Not visible	Not measured	—	Not visible	Not measured	—	$10.68 \times 10^1$	$2.70 \times 10^1$	79.8
Mg no. 2 - 0.2	Not visible	Not measured	—	Not visible	Not measured	—	$3.39 \times 10^2$	$2.50 \times 10^1$	314
Mg no. 7 - 0.025	—	—	—	—	—	—	—	—	—
Mg no. 6 - 0.1	—	—	—	—	—	—	—	—	—
Mg no. 3 - 0.2	—	—	—	—	—	—	—	—	—
Specimen Identification Crack Length	After Crack Extension	After Crack Extension Background	Difference	After Extension and PMB Background	After Extension and PMB Background	Difference	After Extension, PMB, Flexing and Chem Stripper Measurement	After Extension, PMB, Flexing and Chem Stripper Background	Difference
Mg no. 8 - 0.025	—	—	—	—	—	—	—	—	—
Mg no. 1 - 0.1	—	—	—	—	—	—	—	—	—
Mg no. 2 - 0.2	—	—	—	—	—	—	—	—	—
Mg no. 7 - 0.025	$7.91 \times 10^0$	$1.57 \times 10^0$	6.34	Not measured	$3.05 \times 10^2$	$1.51 \times 10^2$	$6.56 \times 10^2$	$4.67 \times 10^2$	189
Mg no. 6 - 0.1	$11.56 \times 10^0$	$2.31 \times 10^0$	9.25	Not measured	$2.83 \times 10^2$	$1.13 \times 10^2$	$3.73 \times 10^2$	$1.68 \times 10^2$	205
Mg no. 3 - 0.2	$11.40 \times 10^0$	$2.70 \times 10^0$	8.7	Not measured	$3.02 \times 10^2$	$1.42 \times 10^2$	$4.25 \times 10^2$	$1.53 \times 10^2$	272

Notes: All measurements were obtained with FPI.  
All measurements are in units of foot-lamberts.

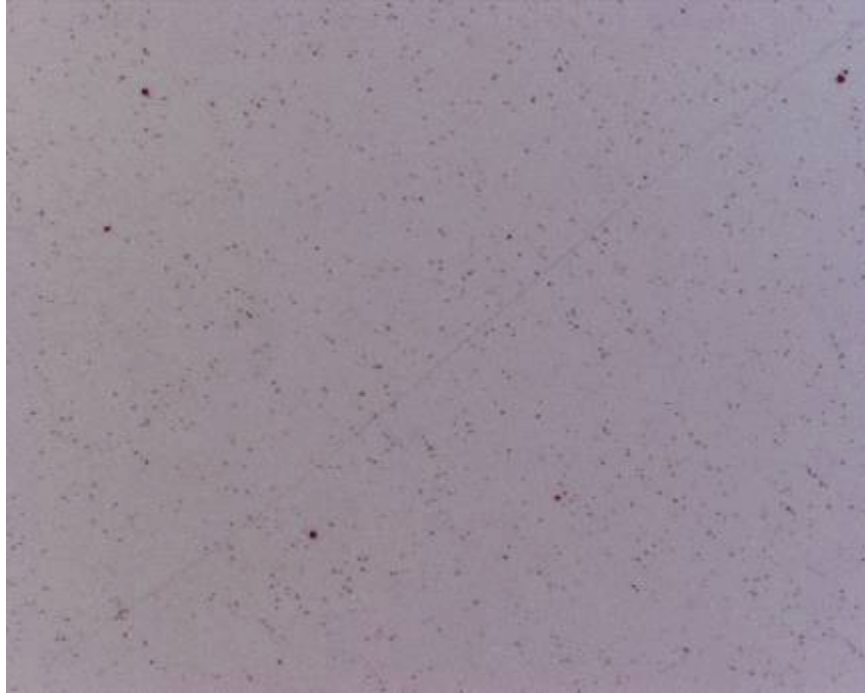


Figure 19. Magnesium bar no. 2 with a 0.2-in crack length.

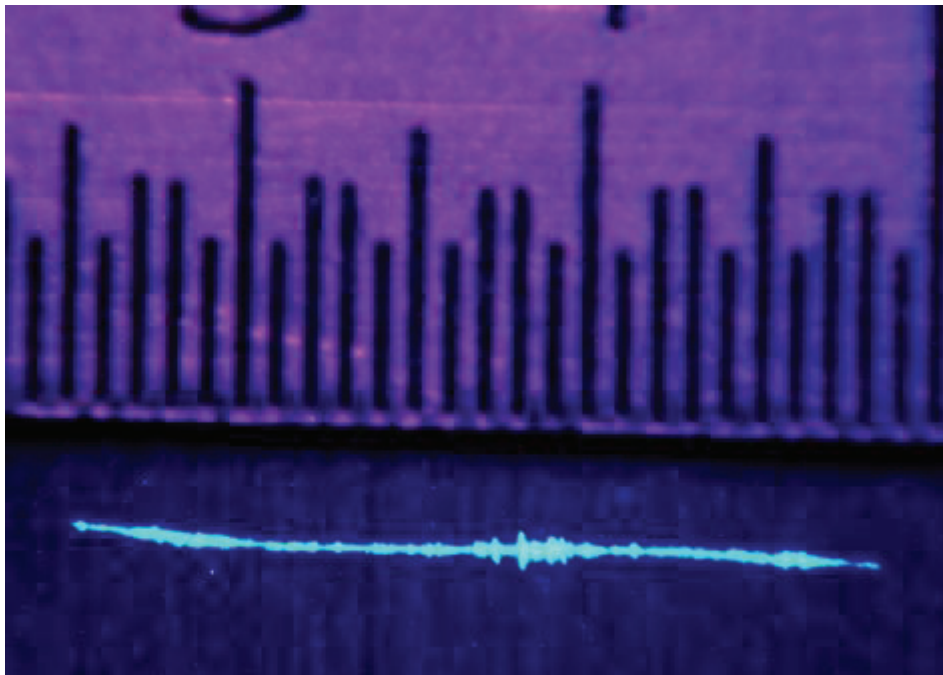


Figure 20. FPI micrograph of cracked Mg bar no. 2 after the crack was initiated and extended to the desired length.

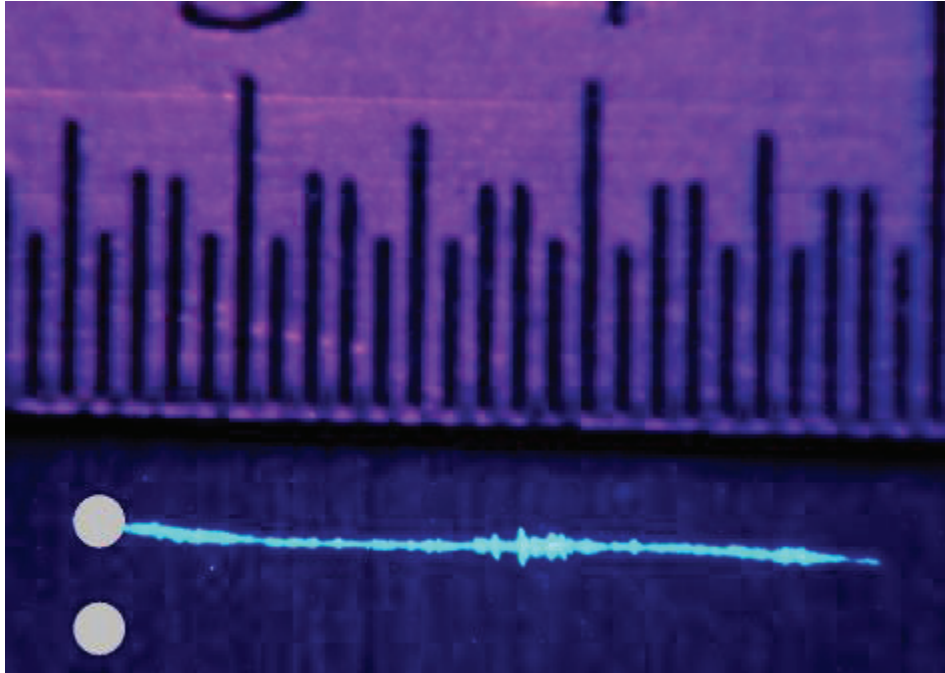


Figure 21. FPI micrograph of cracked Mg bar no. 2 depicting the typical locations of the light measurements. The top spot is the brightness of the crack, and the bottom spot (below the crack) is where the background reading was taken.

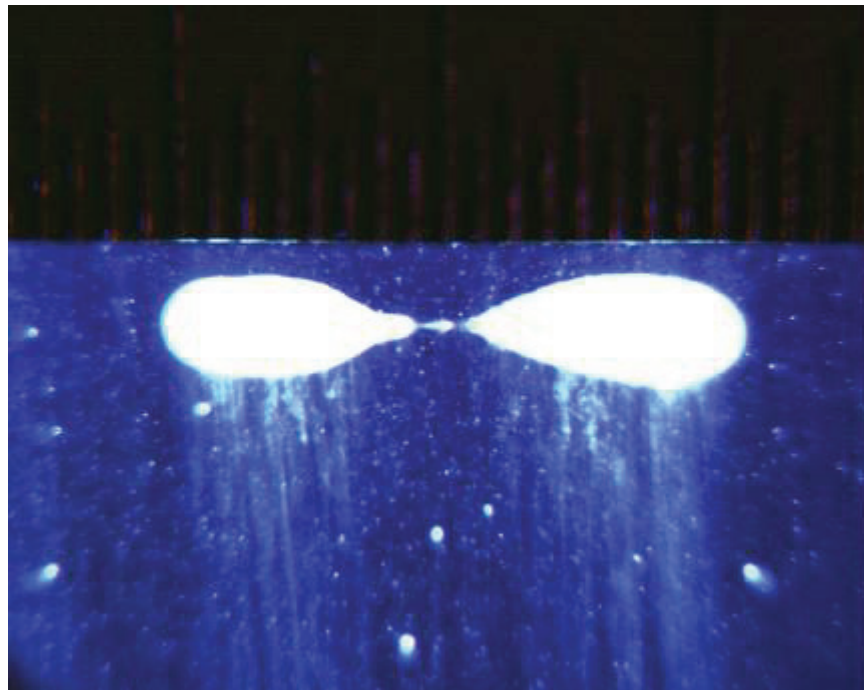


Figure 22. FPI micrograph of cracked Mg bar no. 2 after the Tagnite coating.

would certainly affect the capillary action of the penetrant. The increase in the overall signal from the indications far outweighed the increased background signal, and the result was clear, bright indication of the cracks. No brightness values were recorded after the coating system had been applied to the bars, since no indications could be visually observed. The typical FPI visual results after coating are shown in figure 23. No crack can be observed, and extreme background fluorescence from the paint absorbing penetrant is evident. After extension of the cracks under the coating system, FPI revealed that the cracks became visible. These indications were not nearly as bright as the baseline values, and the background was much higher due to the absorption of the penetrant by the coating system. Figure 24 depicts the typical visual FPI micrographs after crack extension under the coating system. No brightness measurements were recorded after PMB because zero indications were observed during FPI. Paint-stripper processing did not alleviate this condition and the cracks had to be mechanically flexed to dislodge the plastic media from the cracks. Figure 25 represents the typical FPI results after the crack was mechanically flexed to dislodge the plastic media. The brightest measurements were generally yielded from the extended bars after the paint was chemically stripped. However, these bars were flexed, and it is difficult to reliably assess the effect that mechanical flexing had on the characteristics of the crack that yielded the initial brightness, regardless of the fact that the crack length wasn't changed during flexing. Figure 26 depicts the visual FPI results after mechanical flexing of this group.

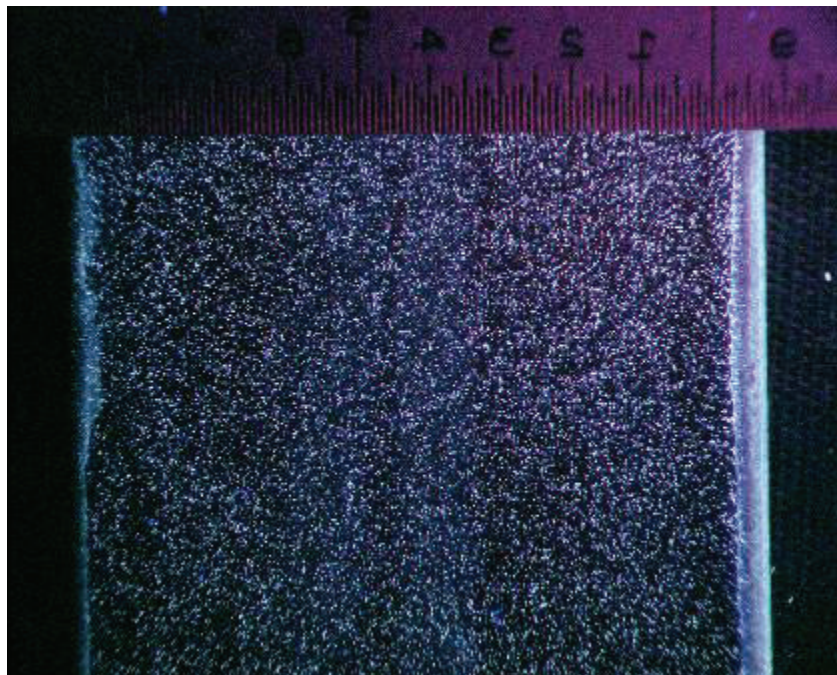


Figure 23. FPI micrograph of cracked Mg bar no. 2 after the application of the coating system. No crack can be observed, and the absorption of the penetrant by the coating is evident.



Figure 24. FPI micrograph of cracked Mg bar nos. 3, 6, and 7 after crack extension under the coating system. Cracks can be observed; however, the absorption of the penetrant by the coating is still evident.

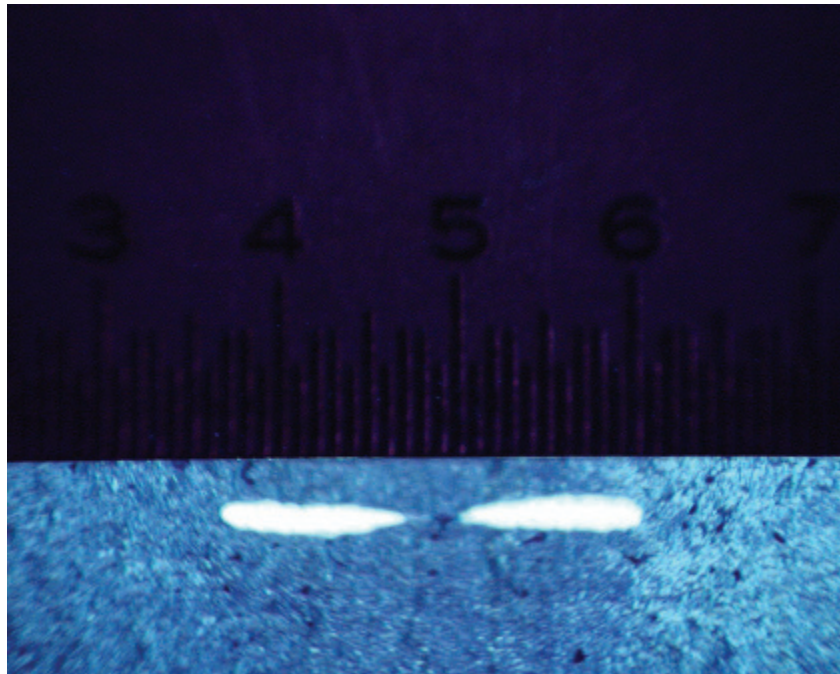


Figure 25. Typical FPI results after PMB, chemical processing, and mechanical flexing to remove the plastic media from within the cracks. Results shown for Mg bar no. 2 after soaking in paint stripper ~24 hr.

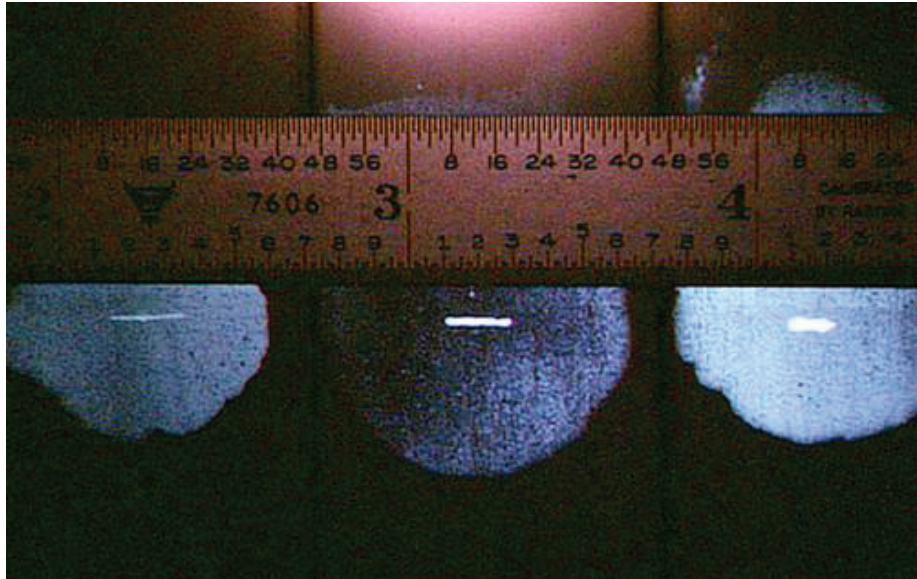


Figure 26. Typical FPI results after crack extension under the coating, PMB, mechanical flexing, and chemical-stripper processing. Results shown for Mg bar nos. 3, 6, and 7 after soaking in paint stripper ~24 hr.

#### 11.4 Steel

MPI was the NDI method evaluated for crack detection in steel. Since a crack does not have to be open to the surface to be detected with MPI, the coating on the steel bars did not undergo PMB or chemical stripping like the other bars. Multiple layers of paint were applied, and MPI was performed after each layer until no cracks could be observed using the standard MPI parameters. The MPI results for steel can be observed in table 13. A typical fatigue crack generated in steel is depicted in figure 27. Initially, FPI was performed to compare the steel with the rest of the materials. The typical visual FPI results on the steel bars can be observed in figure 28. Figure 29 depicts the areas where the light measurements and the background measurements were recorded. Baseline light measurements were recorded during MPI processing. Figure 30 depicts the typical visual results of the baseline group. After cadmium-plating pretreatment, the MPI-generated light measurements were only slightly less than the initial baseline values. After the first application of the coating system, only half of the cracks could be observed. A 0.2-in crack (the longest crack length) and a 0.1-in crack were two of the observable indications. All three of the measured indications were just barely visible to the eye and could not be photographically recorded. The 0.025-in specimens were immeasurable. Figure 31 presents the typical visual results after the cracks were extended 0.05 in. The results showed that the indications were extremely dim and barely detectable. However, the indications were greater than before the cracks were extended. After the second layer of paint, no indications were observable on any bar (figure 32). To investigate if the specimens would show indications with a higher magnetic field, the flux density was increased to 90 G and then gradually increased to 130 G. No indications were observable even at this extreme flux density.

Table 13. Steel spotmeter measurements.

Specimen Identification Crack Length	Initial Crack Measurement	Initial Crack Background Measurement	Difference	After Pretreatment Measurement	After Pretreatment Background	Difference	After Painting Measurement	After Painting Background	Difference
ST no. 1 – 0.025	$4.63 \times 10^0$	$1.42 \times 10^{-1}$	4.488	$4.68 \times 10^0$	$4.33 \times 10^{-1}$	4.247	Not visible	Not measured	—
ST no. 4 – 0.090	$5.89 \times 10^0$	$1.25 \times 10^{-1}$	5.765	$4.67 \times 10^0$	$2.55 \times 10^{-1}$	4.415	$8.5 \times 10^{-1}$	$4.3 \times 10^{-1}$	0.42
ST no. 5 – 0.185	$7.48 \times 10^0$	$1.49 \times 10^{-1}$	7.331	$4.45 \times 10^0$	$4.81 \times 10^{-1}$	3.969	$8.5 \times 10^{-1}$	$4.4 \times 10^{-1}$	0.41
ST no. 3 – 0.030	$5.12 \times 10^0$	$1.71 \times 10^{-1}$	4.949	$5.63 \times 10^0$	$7.80 \times 10^{-1}$	4.85	Not visible	Not meas.	—
ST no. 2 – 0.100	$6.18 \times 10^0$	$1.38 \times 10^{-1}$	6.042	$4.08 \times 10^0$	$3.08 \times 10^{-1}$	3.772	Not visible	Not measured	—
ST no. 6 – 0.185	$7.20 \times 10^0$	$1.48 \times 10^{-1}$	7.052	$3.50 \times 10^0$	$1.80 \times 10^{-1}$	3.32	$8.3 \times 10^{-1}$	$6.2 \times 10^{-1}$	0.768

Specimen Identification Crack Length	After Crack Extension Measurement	After Crack Extension Background	Difference	After 2nd Coating Applied Measurement	After 2nd Coating Applied Background	Difference	Steel Bar Paint Thickness 1st Coat (mil)	Steel Bar Paint Thickness Total (mil)
ST no. 1 – 0.025	—	—	—	Not visible	Not measured	—	3.9	9.6
ST no. 4 – 0.090	—	—	—	Not visible	Not measured	—	3	7.8
ST no. 5 – 0.185	—	—	—	Not visible	Not measured	—	3.4	8.4
ST no. 3 – 0.030	$1.43 \times 10^0$	$0.55 \times 10^0$	0.88	Not visible	Not measured	—	3.1	8.2
ST no. 2 – 0.100	$1.67 \times 10^0$	$0.98 \times 10^0$	0.69	Not visible	Not measured	—	3.8	9.1
ST no. 6 – 0.185	$2.30 \times 10^0$	$0.69 \times 10^0$	1.61	Not visible	Not measured	—	3	8.2

Notes: All measurements were obtained with MPI  
All measurements are in units of foot-lamberts.



Figure 27. Bar no. 3 after initiation and crack extension—typical fatigue crack generated in steel.

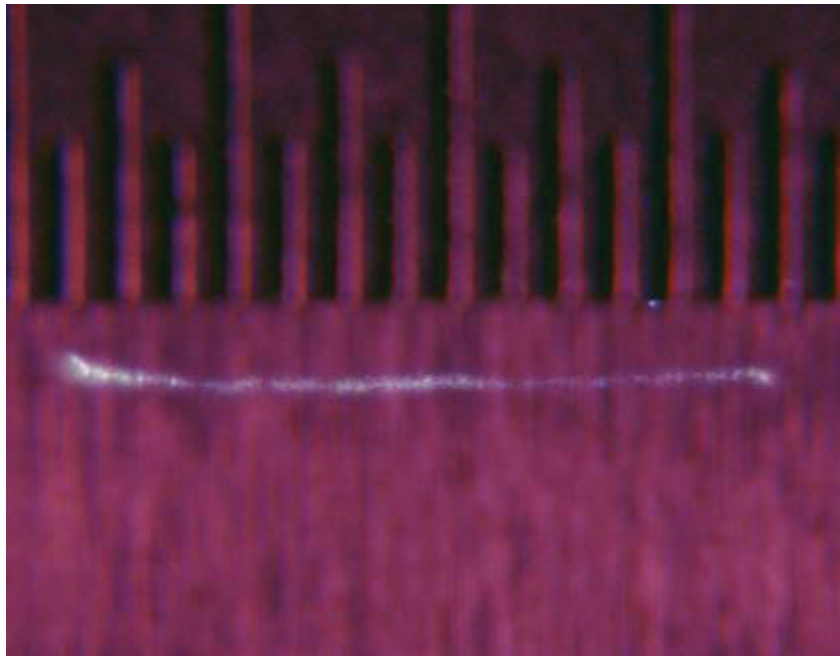


Figure 28. Steel bar no. 6 after initial crack extension—0.2 in crack. Typical FPI visual results on steel fatigue cracks.

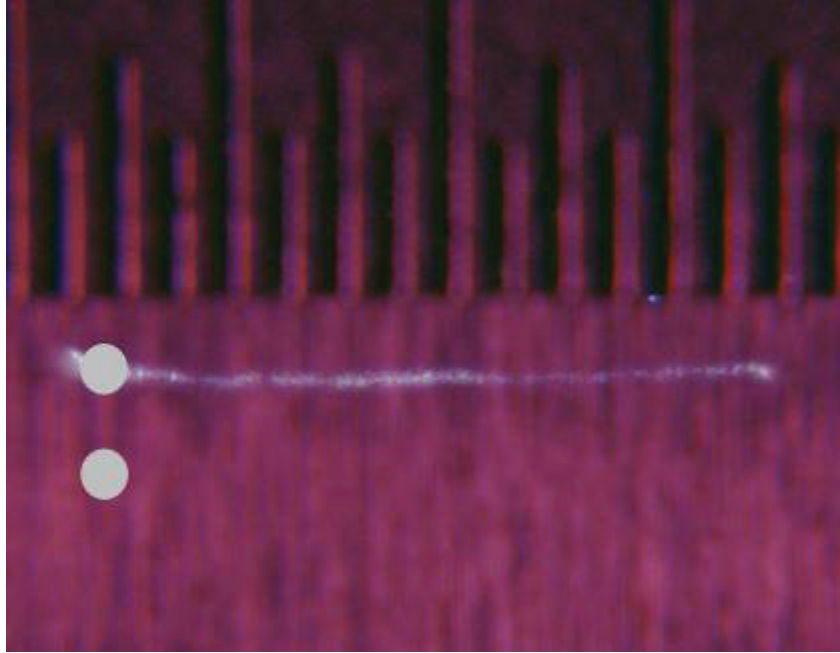


Figure 29. Typical FPI micrograph of steel showing the areas where brightness measurements were taken on this bar. The top dot (on the crack) is the crack brightness measurement location. The bottom dot (below the crack) is the background measurement location.

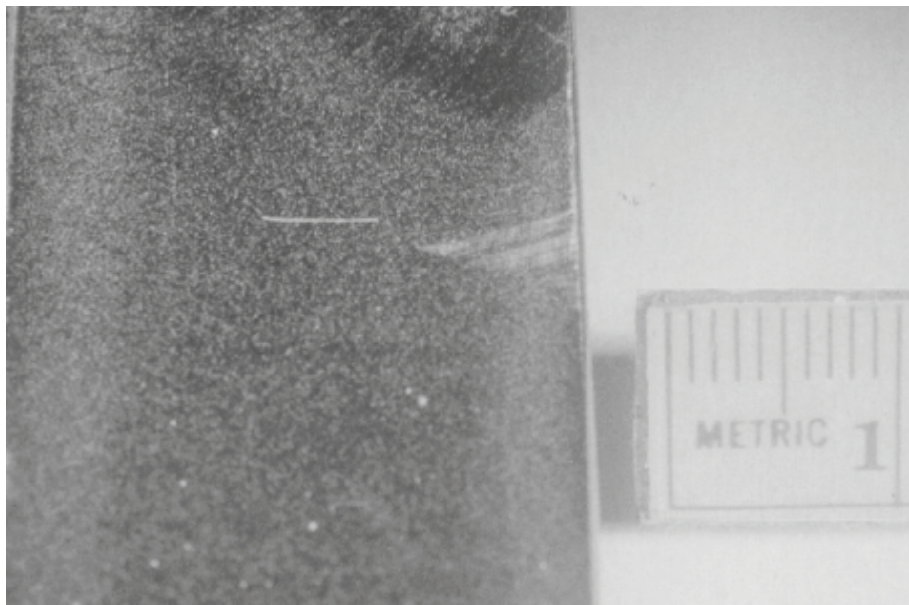


Figure 30. Bar no. 6 after the initiation and crack extension. Typical baseline visual MPI micrograph on steel.

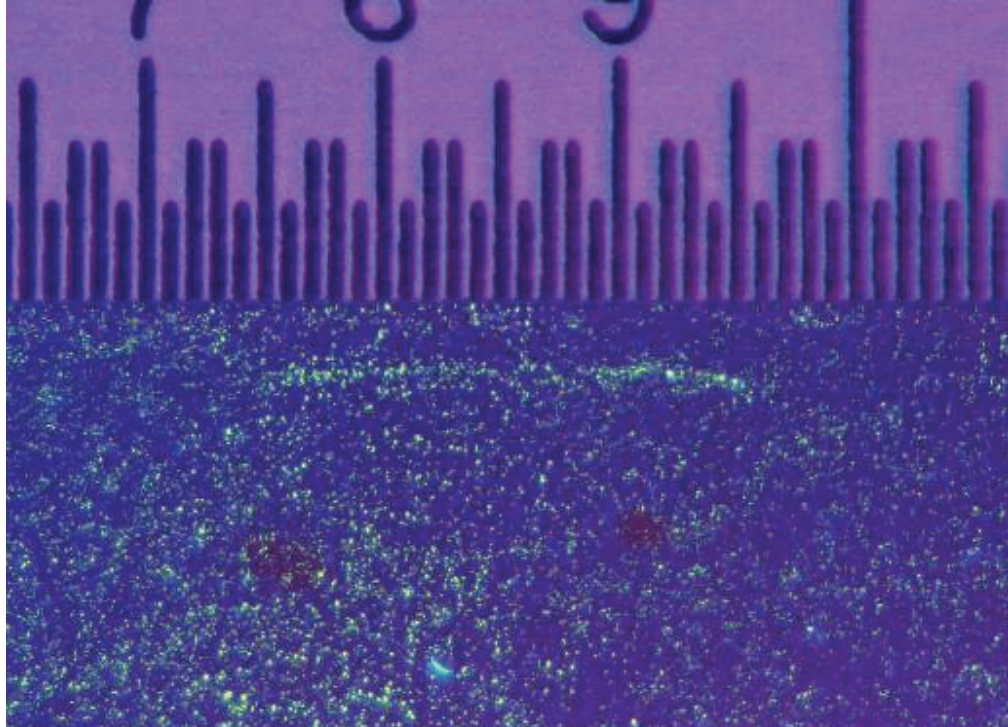


Figure 31. Bar no. 6 after the 0.050-in crack extension. Typical visual MPI micrograph after crack extension.

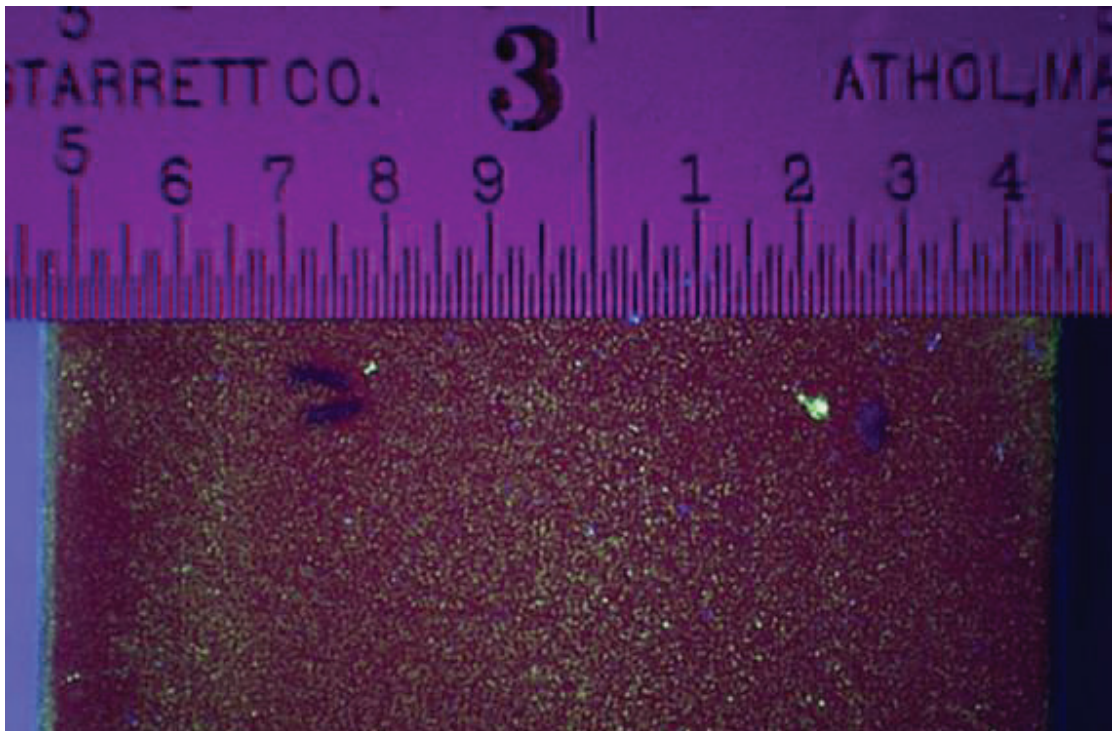


Figure 32. Typical visual MPI micrograph after the application of the second layer of paint. All traces of the crack indication are gone.

---

## **12. Discussion**

---

### **12.1 Scope**

It was evident within the results that this study was overly aggressive in scope. The creation and use of the same set of specimens to evaluate the effect of NDI performed over paint while subsequently using these same specimens for the evaluation of PMB and chemical paint stripping produced coupled effects. The effect of one process on the value of the light measurement could not be completely separated from the effects of the subsequent processes. For instance, it was assumed that Type V PMB would be sensitive enough to remove just the topcoat and leave the primer unaffected. The cured paint conditions proved this assumption incorrect. It was also assumed that this PMB process would effectively remove the paint system and leave an adequately cleaned crack for FPI. The soft Type V PMB penetrated, wedged, and masked the cleaned cracks, especially those which were longer and wider. The subsequent chemical-stripping-process evaluation was affected by this lodged Type V plastic media. It was thought beforehand that any residual effect of the paint on the measured light value would be mostly removed by the PMB and completely removed by the chemical-stripping process, yielding the initial brightness values (or at least a very close approximation of those values). The results demonstrated that performing FPI over the paint was impossible. Type V media removed the paint but became lodged in the cracks. Even in subsequent chemical stripping, it could not bring back the cracks to their initial condition. The Type V media proved resistant to the chemical stripper. The dislodging of the plastic media from the cracks could only be accomplished by mechanical flexing of the crack. It was also not completely known whether this process was 100% effective. There might exist some residual plastic media within the cracks.

### **12.2 Effect of Performing FPI Over Paint**

Performing FPI of cracks which were painted over proved futile. There existed no path for the penetrant to infiltrate and collect within the cracks, and the paint absorbed a great deal of penetrant, which led to high background fluorescence. FPI performed over paint when the cracks were extended proved only slightly more rational. Although fractures within the coating system resulting from extension of the cracks under the paint could be observed under microscopic examination, sound FPI of these cracks proved impossible. The paint absorbed the penetrant, which resulted in extreme background fluorescence of the entire area. This eliminated any contrast between the crack and the background. This contrast is solely responsible for drawing one's attention and leads to the observation of an indication. Additionally, the paint proved far too flexible to allow substantial amounts of the penetrant to collect within the crack. Essentially, the paint is flexible, and it closes on itself after removal of the stresses that extend or open a crack and fracture the paint. So even though fractures within the paint can be observed under microscopic examination, there exists very little opening for penetrant to flow into the

permanently deformed crack suggesting it is still open under the paint after removal of the stress). A stiffer, less compliant coating system may allow penetrant to collect within a crack; however, the coating system must also not absorb penetrant because that would still have a detrimental effect on the results.

### **12.3 PMB**

The Type V media penetrates and lodges within the cracks of the materials tested. The larger the crack width, the more media becomes lodged. This type of media should not be used prior to FPI, as the cracks are either completely obliterated or greatly reduced in brightness.

### **12.4 Chemical Removal**

This method should have effectively removed the residual paint from the PMB process. Since it was performed after the PMB process, the results were commingled. The stripper could not remove the plastic media, so the cracks were still masked. There is nothing to suggest that the chemical stripper itself causes a detrimental effect on the FPI process. However, since the chemical stripping was not done immediately after the FPI over the paint, it is not known whether chemical stripping could be an effective means of removing paint from cracks like those that were missed during a routine inspection and subsequently painted over.

---

## **13. Conclusions**

---

### **13.1 FPI**

- The process performed over paint is not conducive to revealing sharp, bright indications on materials and crack sizes used within this study. The paint system completely obliterated the indications and absorbed the fluorescent penetrant, which eliminated any contrast between the crack and the background fluorescence.
- The Type V media, although effective at removing the paint system in this study, is soft enough that it lodges within the cracks and significantly reduces the measured brightness of the indications.
- Chemical paint stripping is unable to remove the lodged plastic media from within the cracks.

### **13.2 MPI**

- One layer of the coating system in this study greatly reduced the effectiveness of the inspection technique. Two layers of the coating system completely masked the crack even when MPI was performed with magnetic fields up to 130 G.

---

## 14. References

---

1. ADS-61-PRF. *Aeroautical Design Standard 61*. U.S. Army Aviation and Missile Command: Huntsville, AL, 2001.
2. MIL-A-8625. *Anodic Coatings for Aluminum and Aluminum Alloys* **1993**.
3. SAE-AMS-QQ-P-416. *Plating, Cadmium (Electrodeposited)* **2002**.
4. MIL-P-23377. *Primer Coatings: Epoxy, High Solids* **1994**.
5. MIL-C-64159. *Coating, Water Dispersible Aliphatic Polyurethane, Chemical Agent Resistant* **2002**.
6. ASTM-E-1444. Standard Practice for Magnetic Particle Testing Standard Practice for Magnetic Particle Testing. *Annu. Book ASTM Stand.* **2005**.
7. ASTM-E-1417. Standard Practice for Liquid Penetrant Examination. *Annu. Book ASTM Stand.* **2005**.
8. ASTM-E-1444. Standard Practice for Magnetic Particle Testing. *Annu. Book ASTM Stand.* **2005**.
9. MIL-P-85891. *Plastic Media, for Removal of Organic Coatings* **1998**.

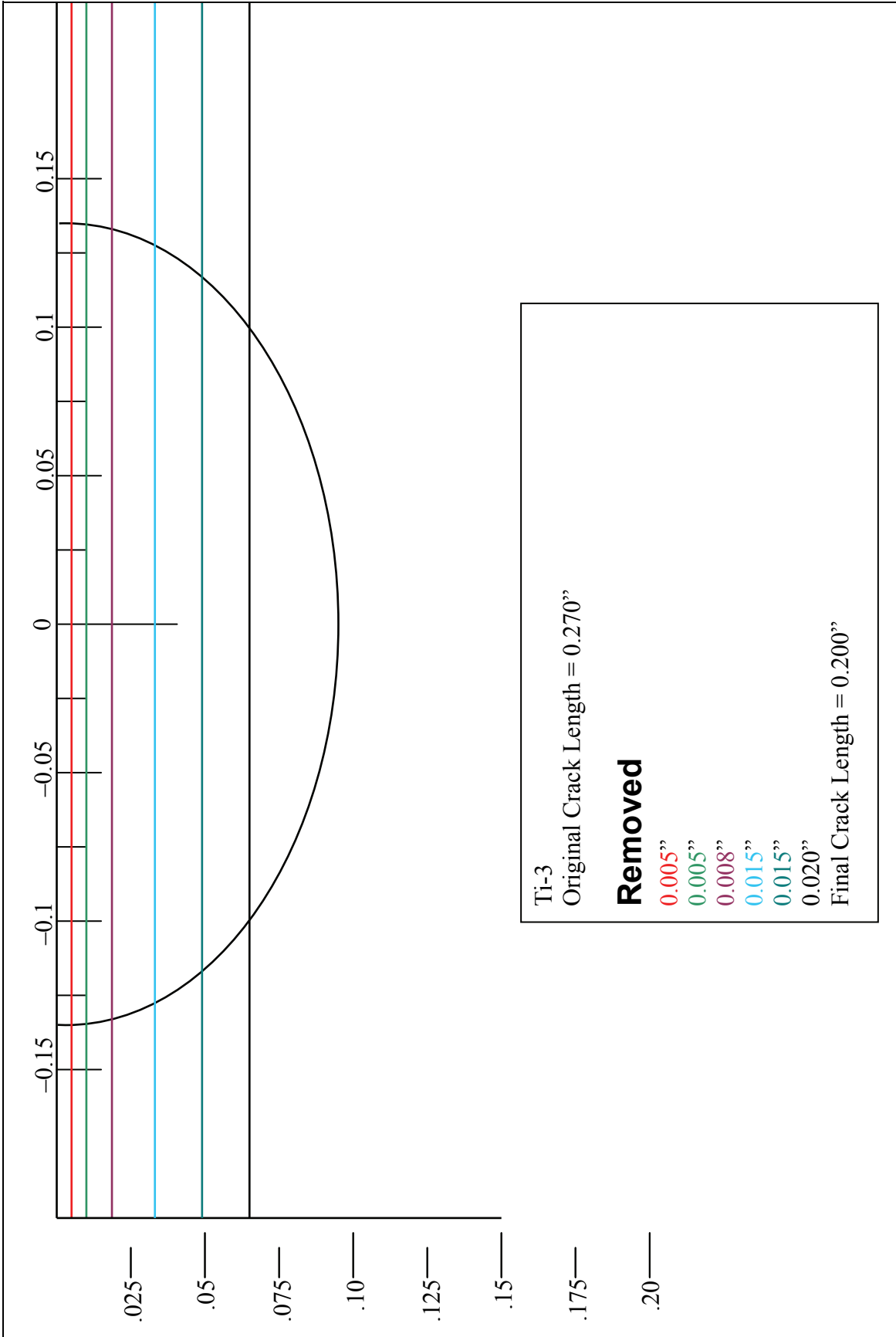
---

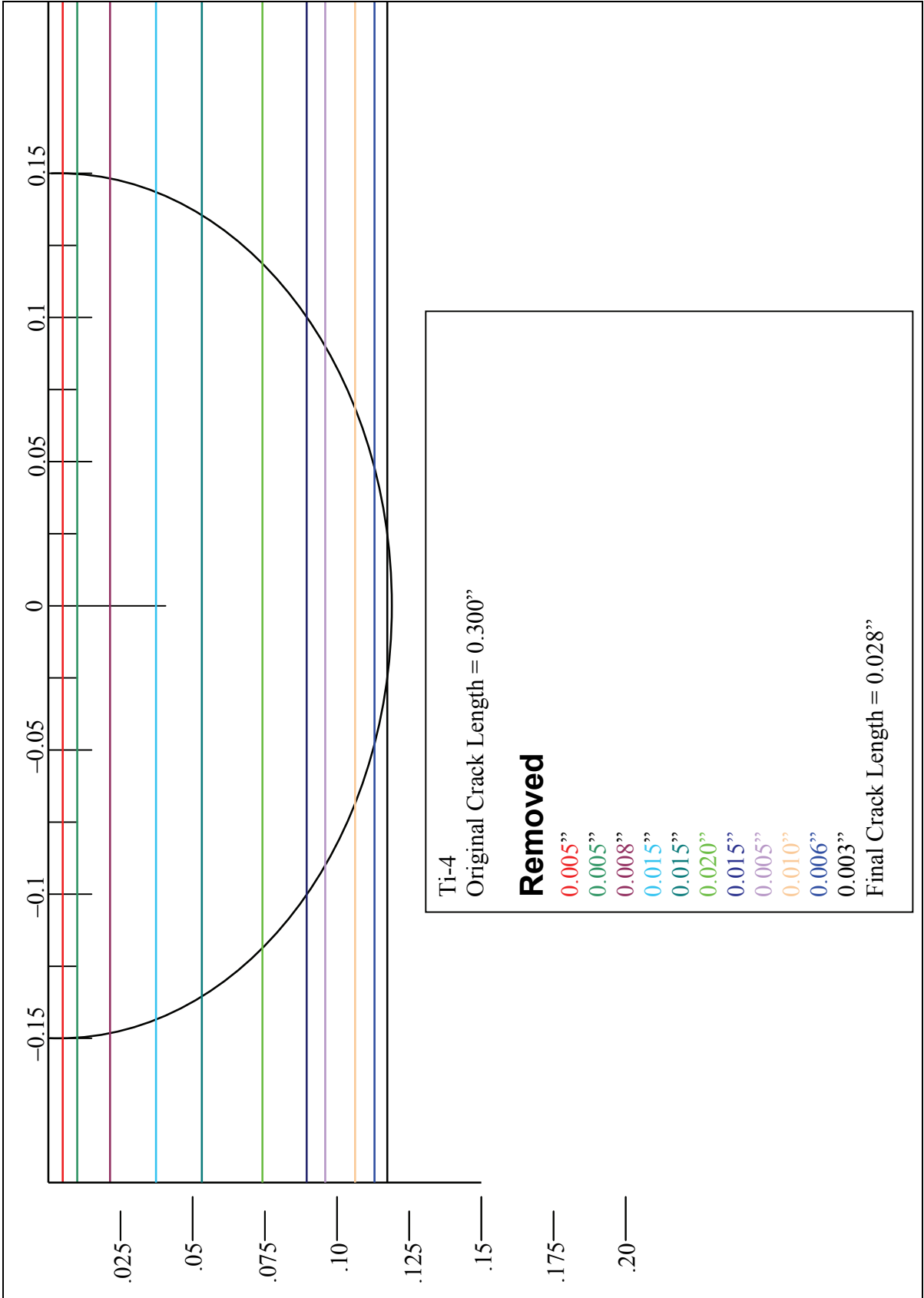
## **Appendix. Schematics of the Incremental Formation of the Specimens**

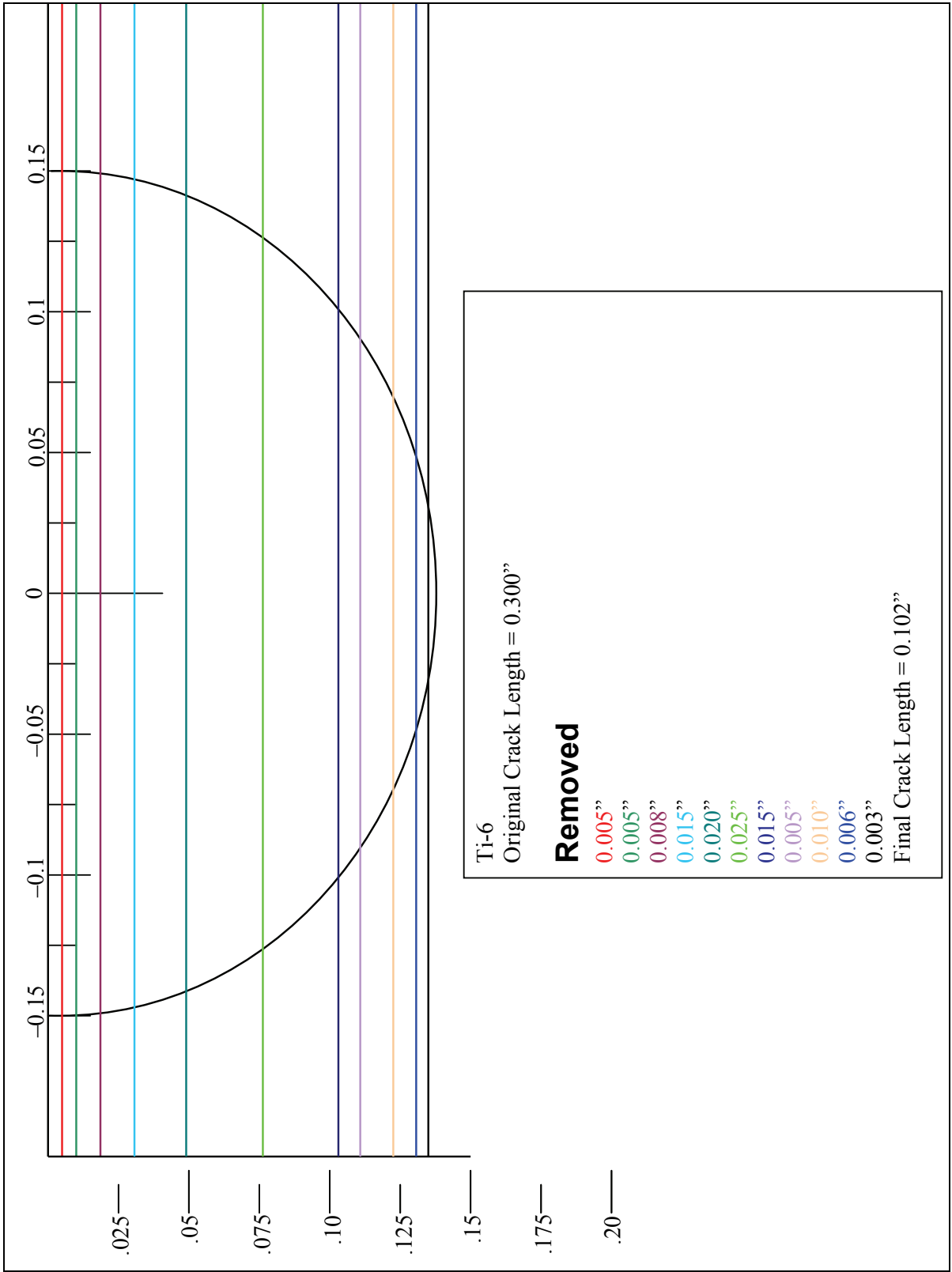
---

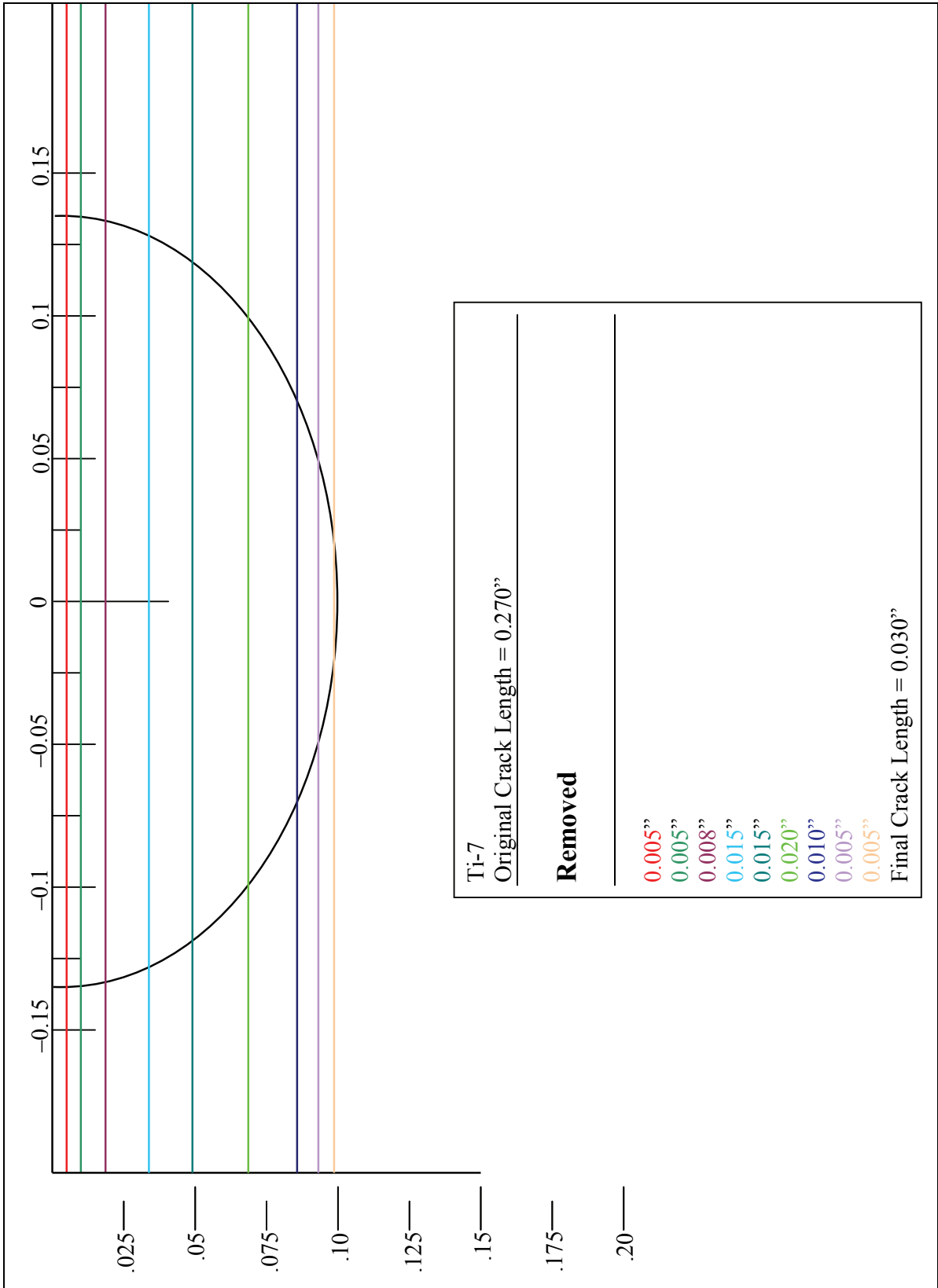
---

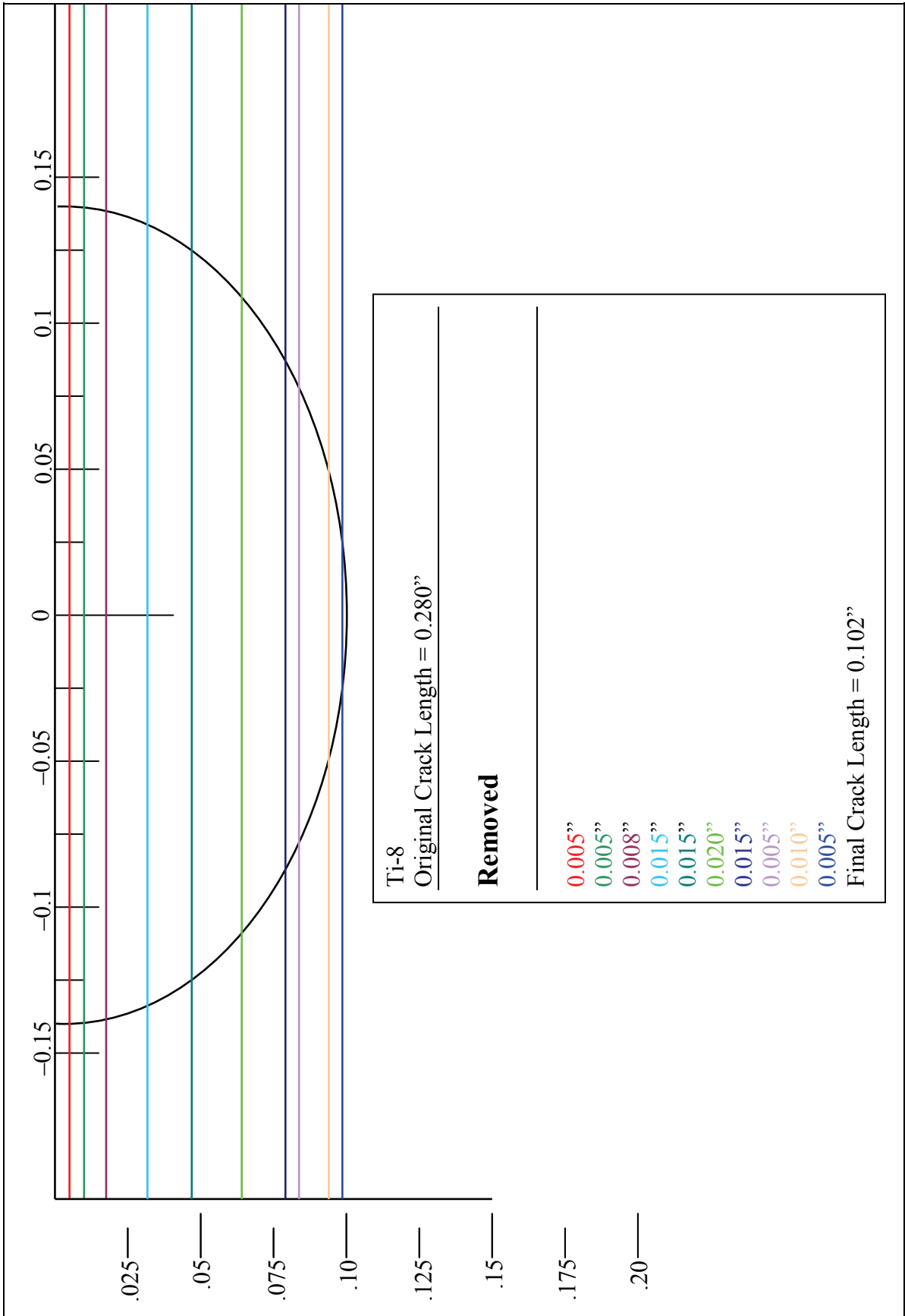
This appendix appears in its original form, without editorial change.

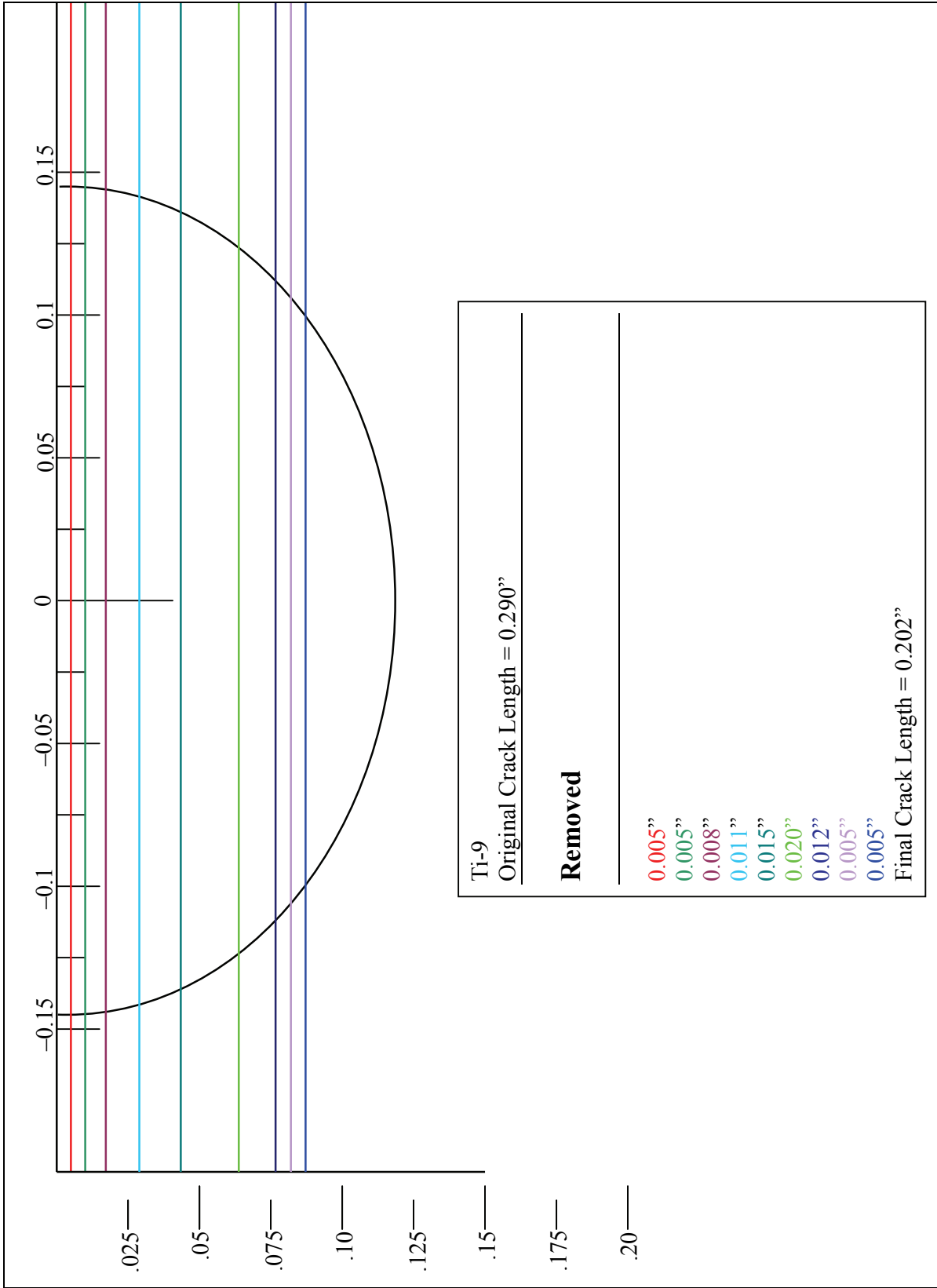


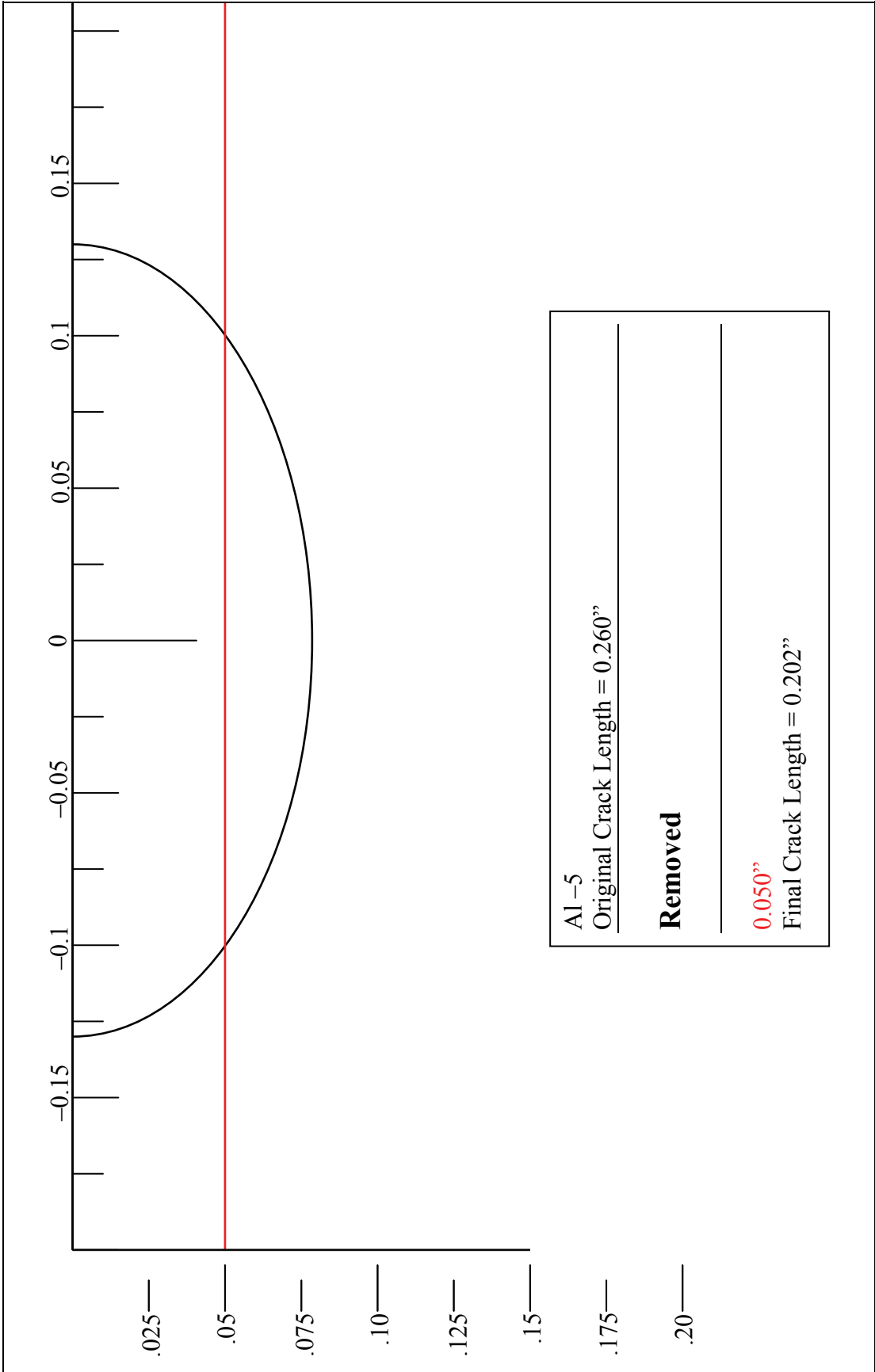


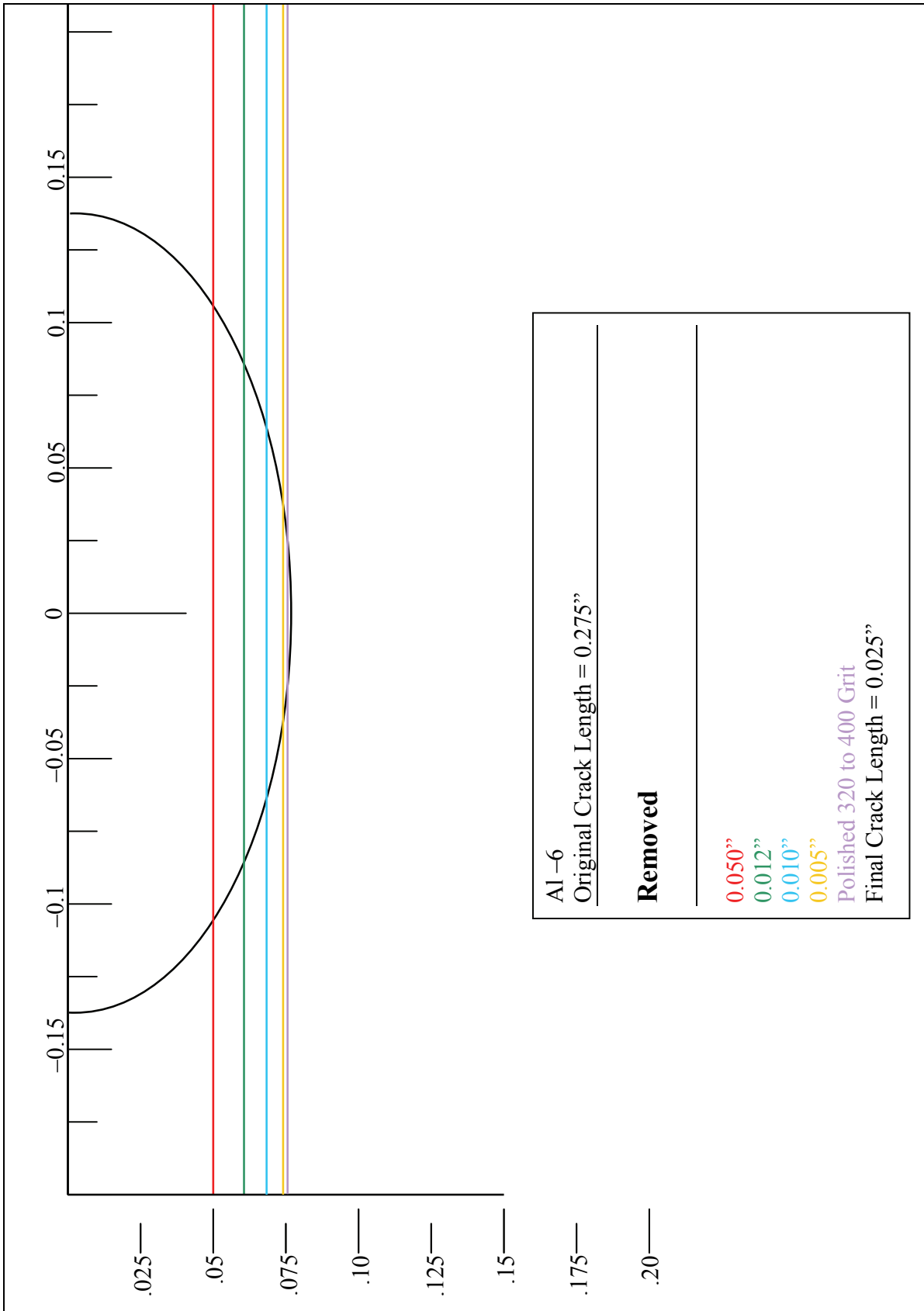


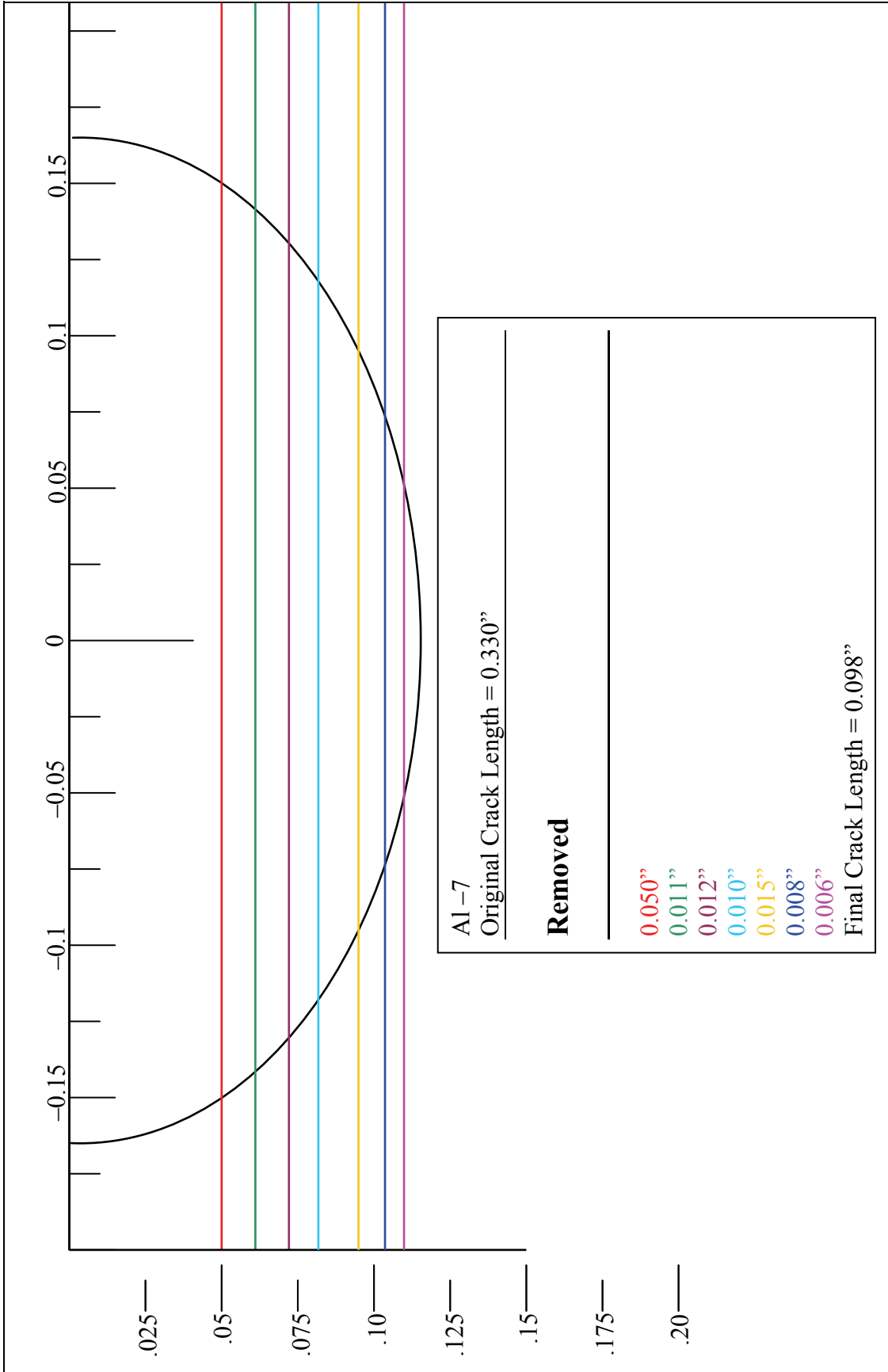


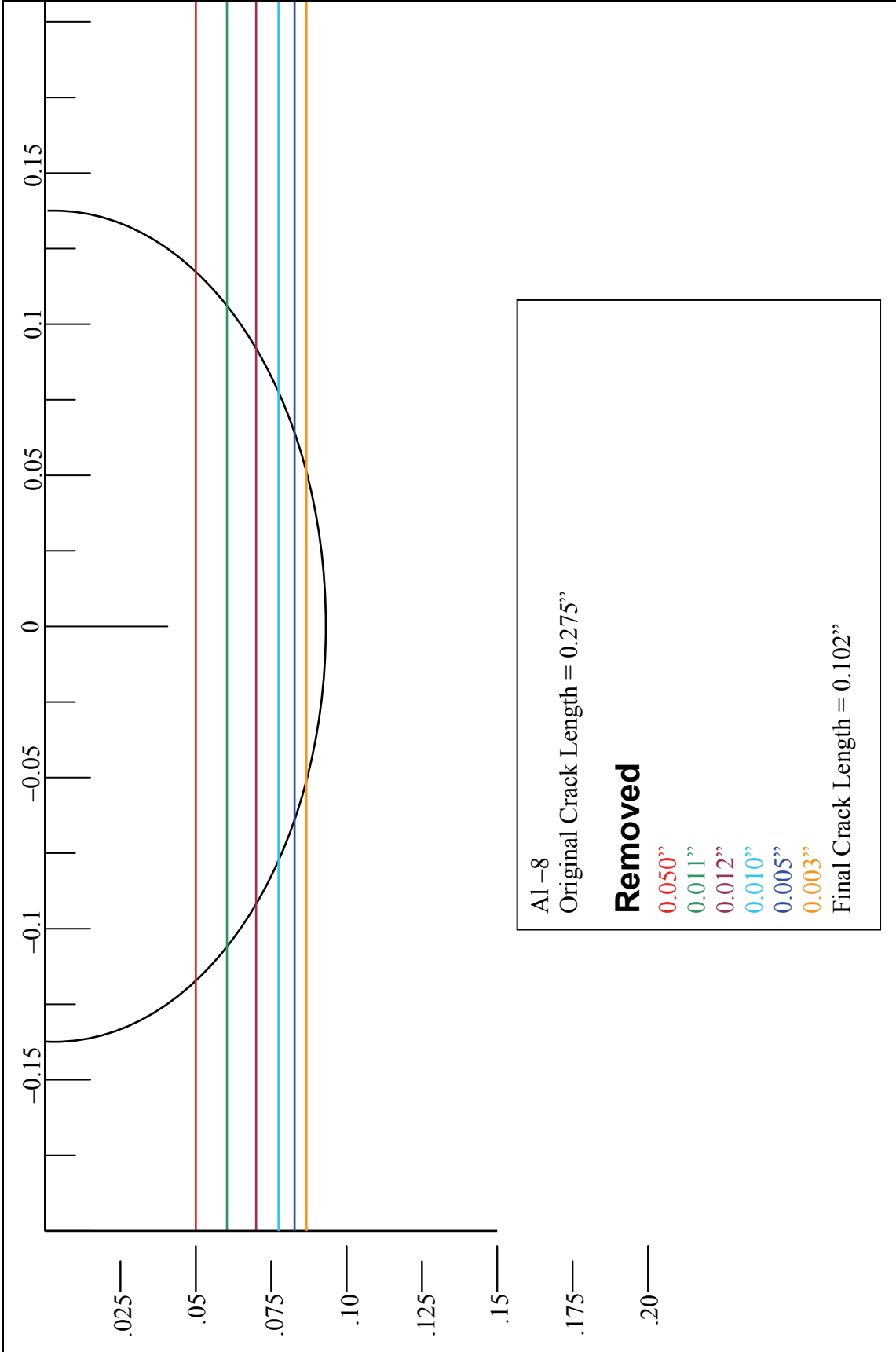


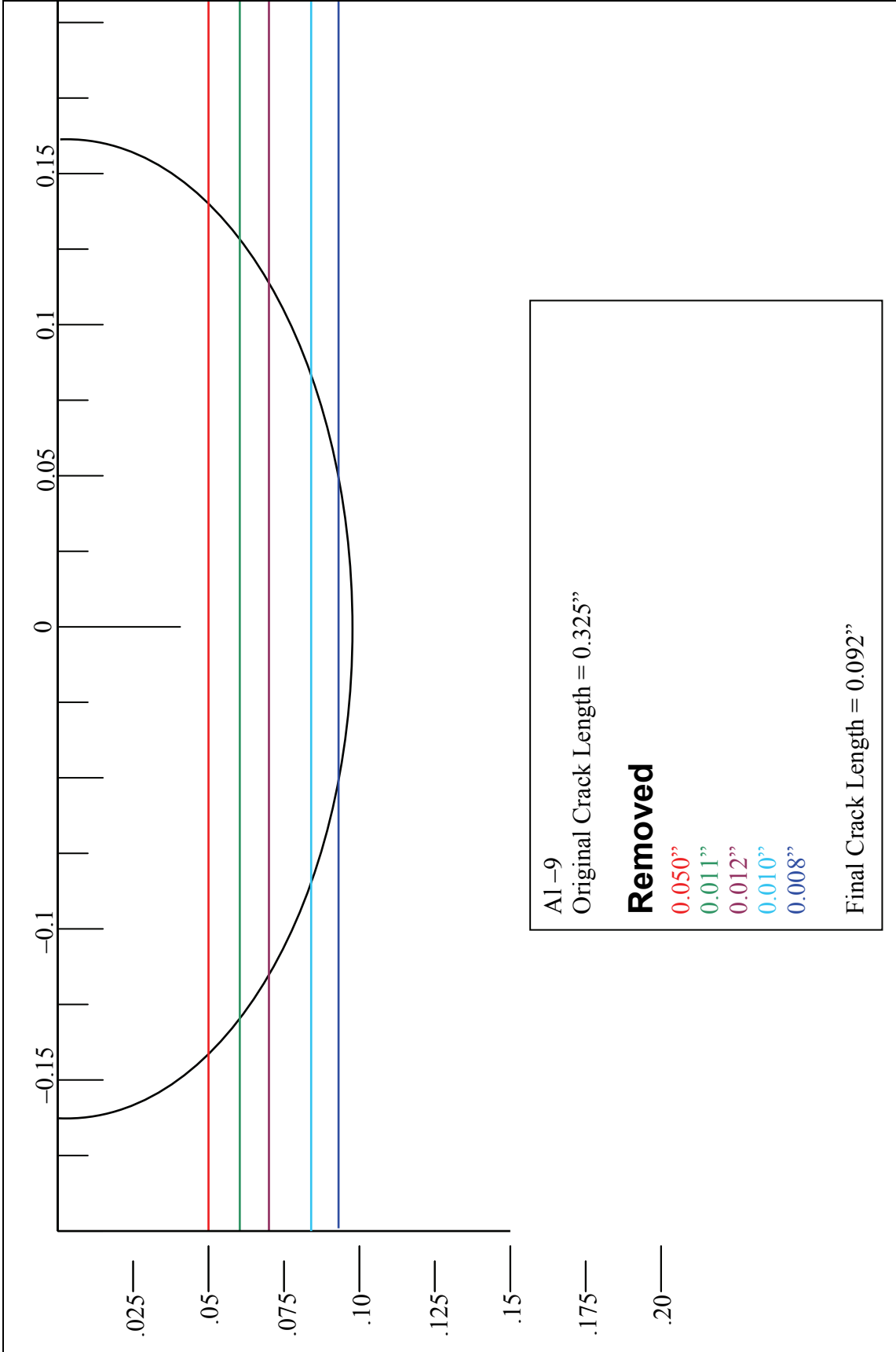


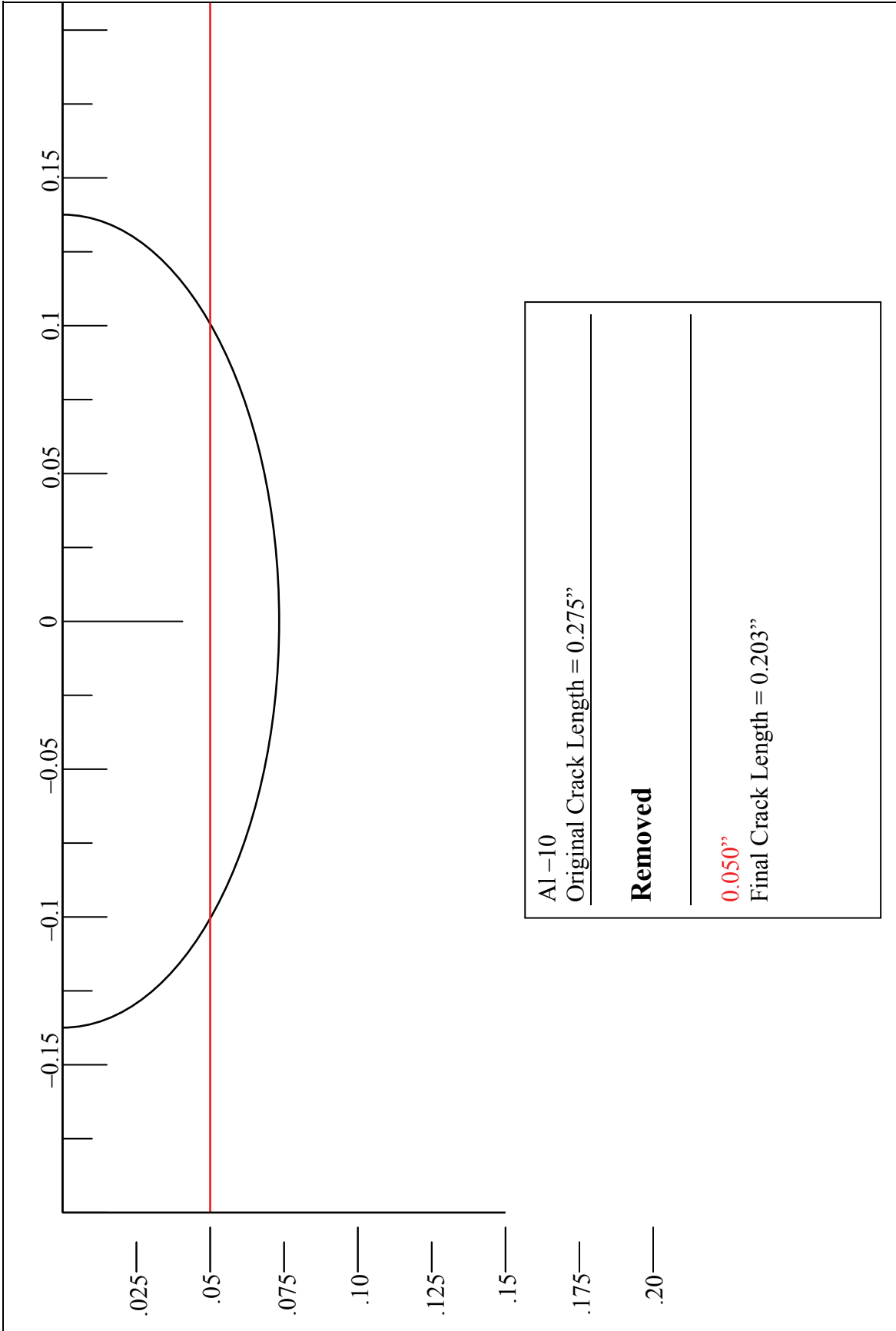


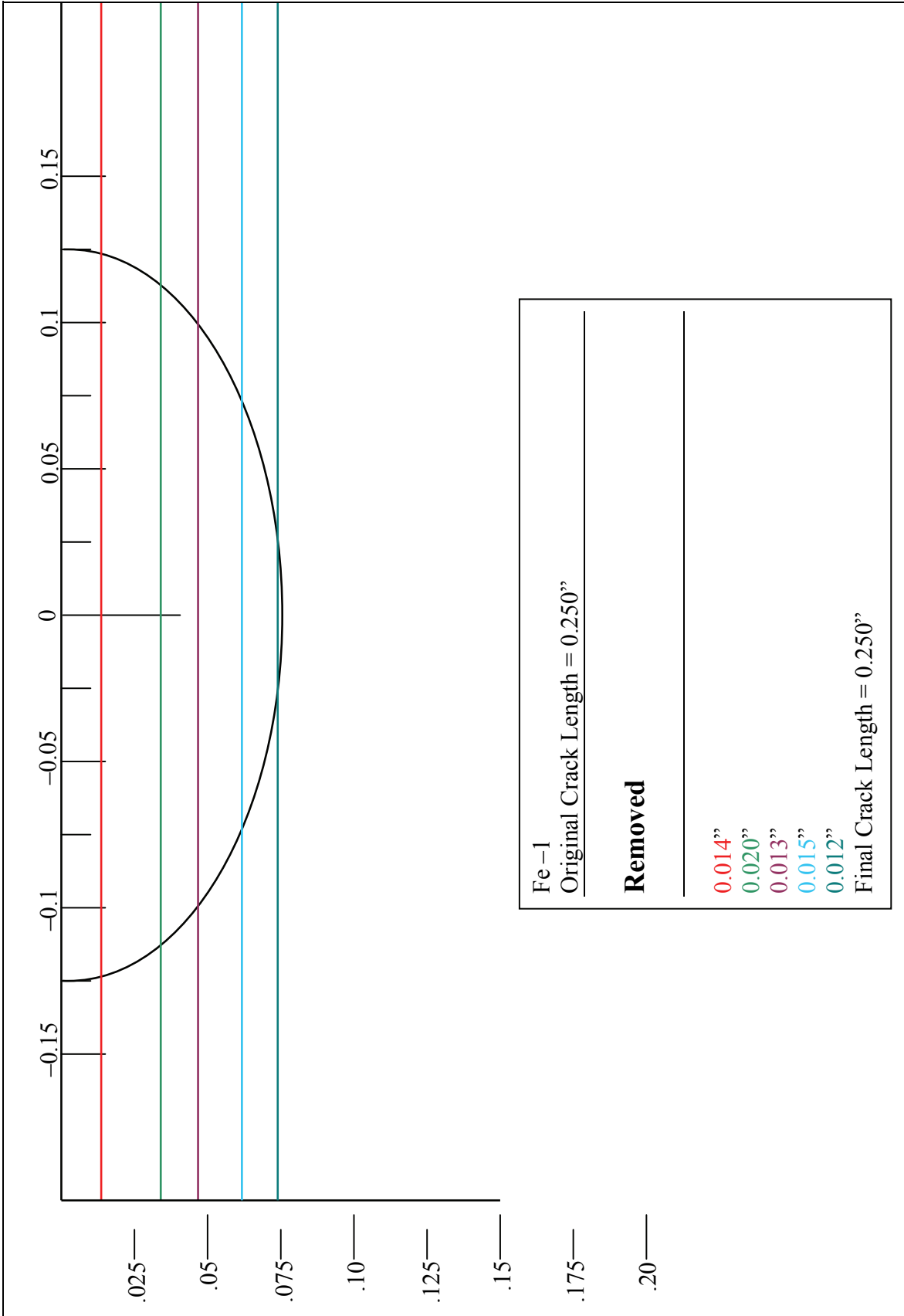


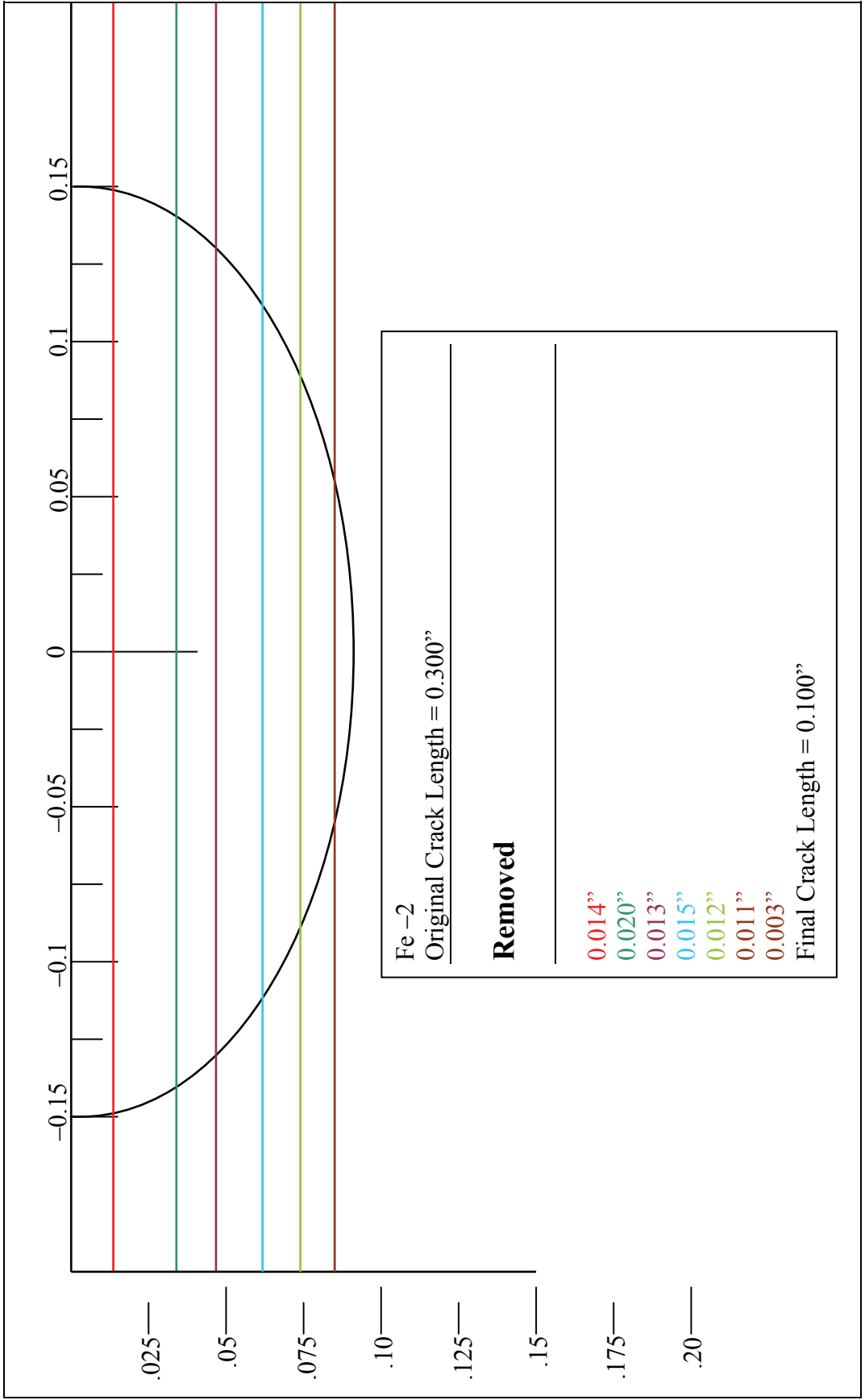


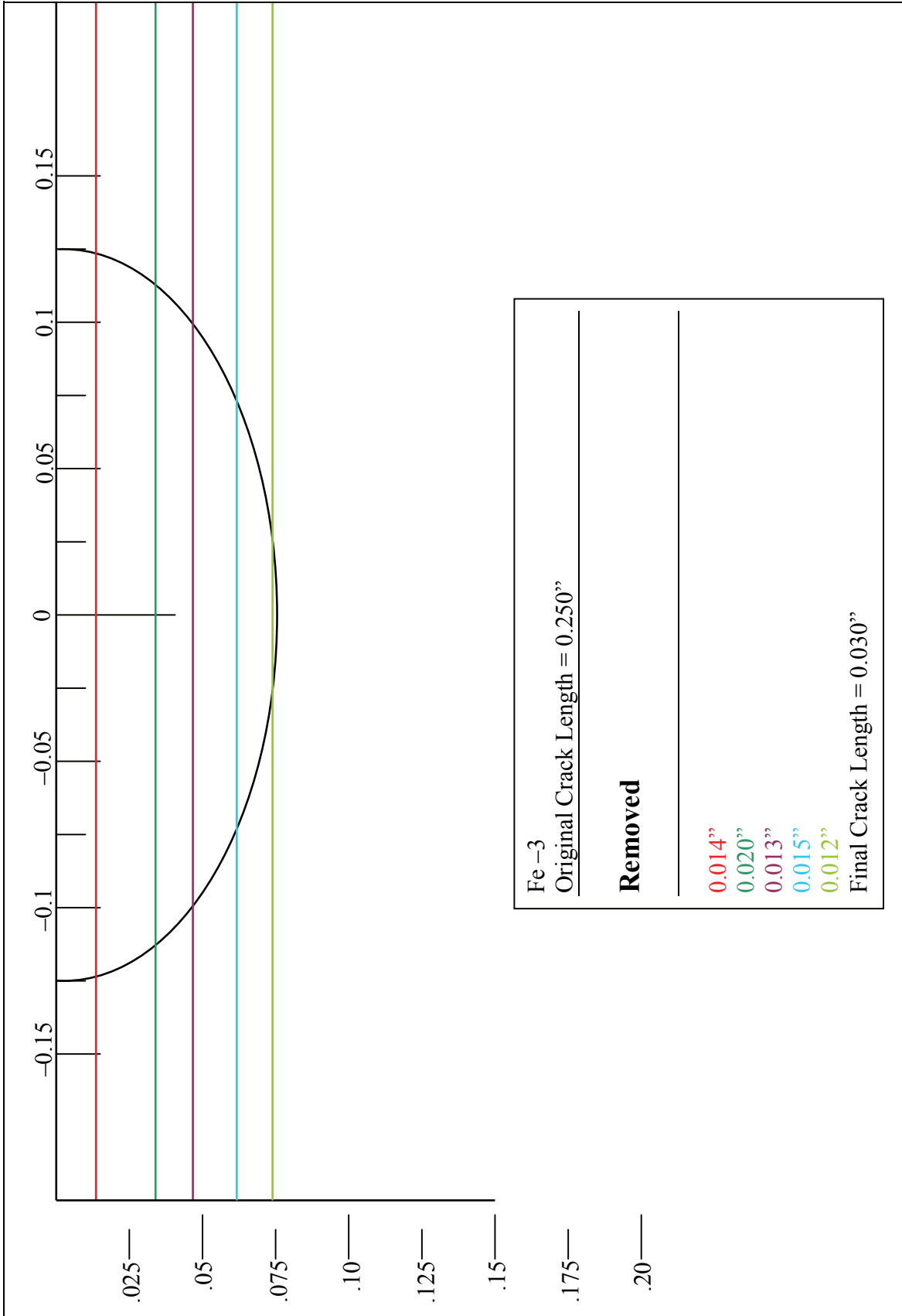


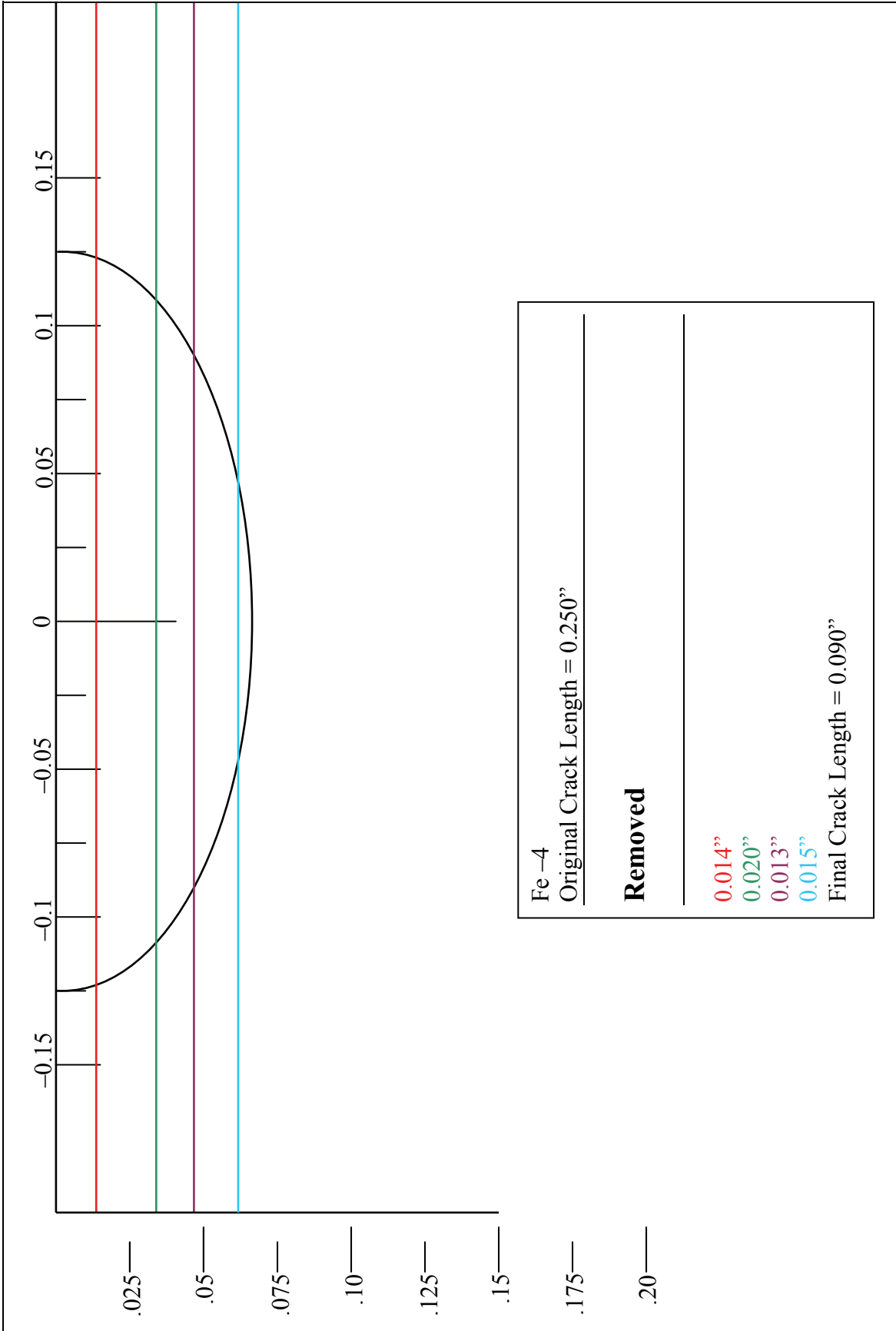


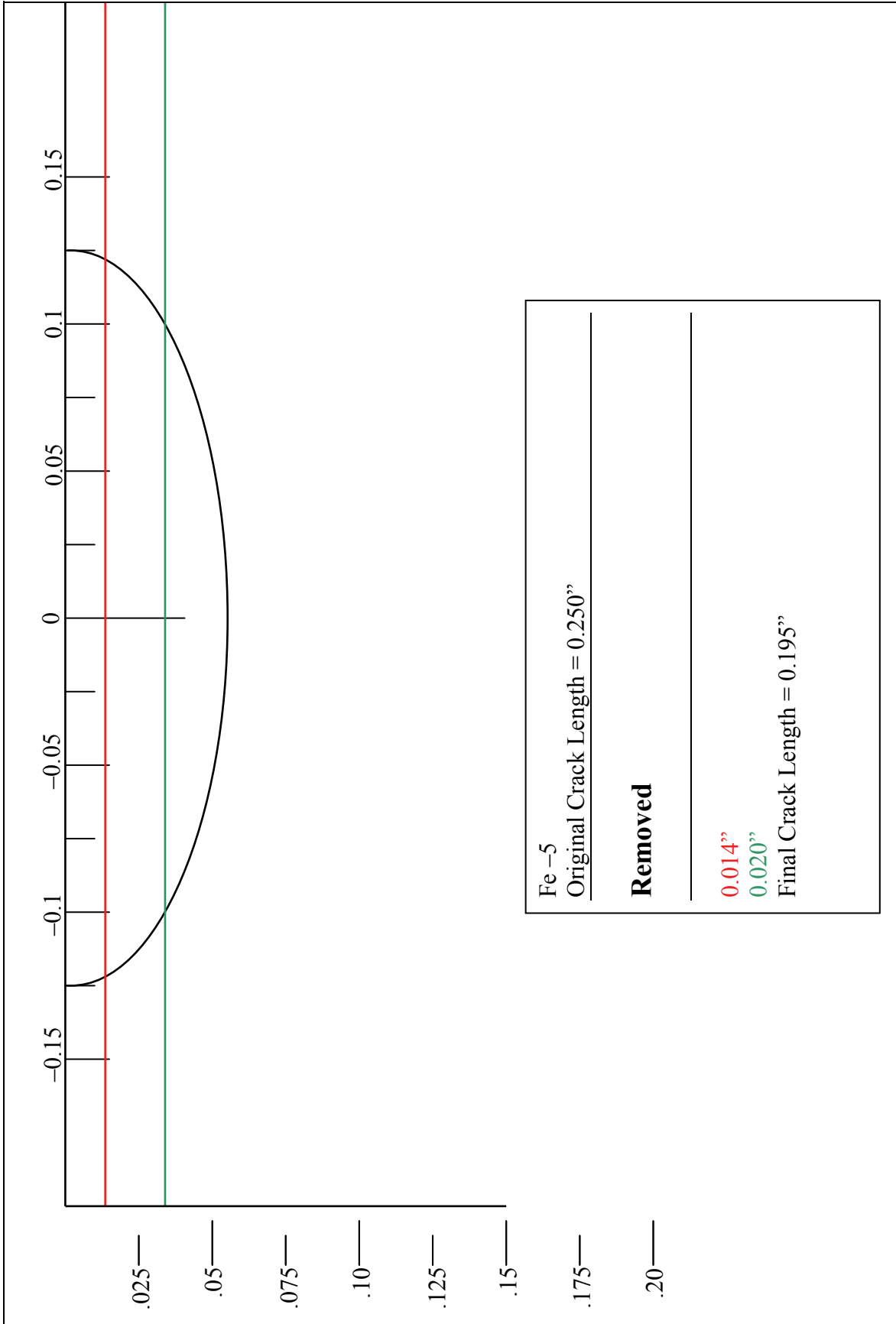


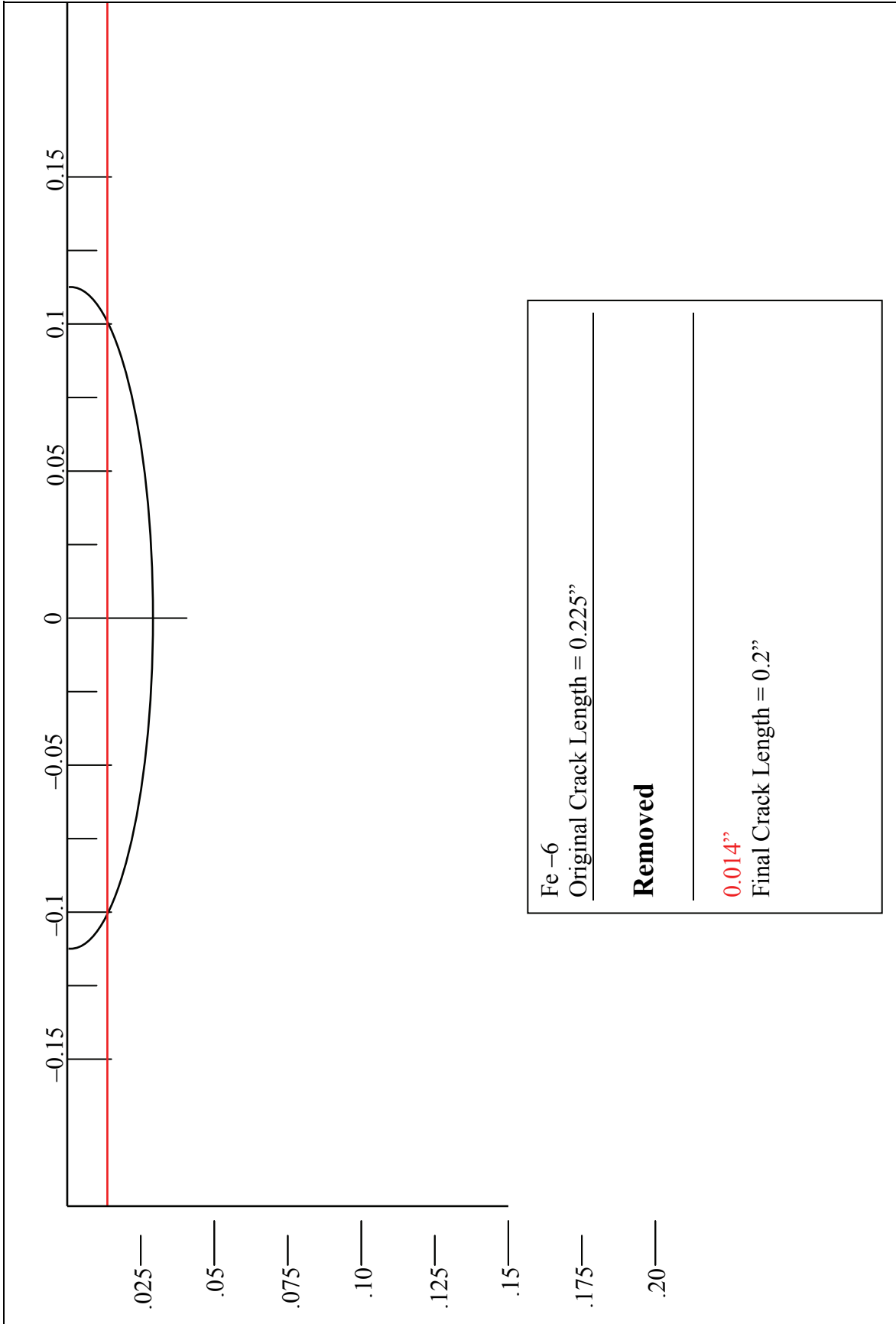












NO. OF  
COPIES ORGANIZATION

1 DEFENSE TECHNICAL  
(PDF INFORMATION CTR  
ONLY) DTIC OCA  
8725 JOHN J KINGMAN RD  
STE 0944  
FORT BELVOIR VA 22060-6218

1 US ARMY RSRCH DEV &  
ENGRG CMD  
SYSTEMS OF SYSTEMS  
INTEGRATION  
AMSRD SS T  
6000 6TH ST STE 100  
FORT BELVOIR VA 22060-5608

1 DIRECTOR  
US ARMY RESEARCH LAB  
IMNE ALC IMS  
2800 POWDER MILL RD  
ADELPHI MD 20783-1197

3 DIRECTOR  
US ARMY RESEARCH LAB  
AMSRD ARL CI OK TL  
2800 POWDER MILL RD  
ADELPHI MD 20783-1197

ABERDEEN PROVING GROUND

1 DIR USARL  
AMSRD ARL CI OK TP (BLDG 4600)

NO. OF  
COPIES ORGANIZATION

ABERDEEN PROVING GROUND

- 2 DIRECTOR  
USAATC  
AMSRD ARL WM MC  
B HARDISKY
  
- 4 DIRECTOR  
USARDECOM  
AMSRD AMR AE F M  
K BHANSALI (2 CPS)  
M KANE (2 CPS)
  
- 2 DIR USARL  
AMSRD ARL WM MC  
S GREENDAHL

INTENTIONALLY LEFT BLANK.